Available online at www.sciencedirect.com
SCIENCE DIRECT®
International Journal of Solids and Structures 42 (2005) 819–853
INTERNATIONAL JOURNAL OF SOLIDS and STRUCTURES
www.elsevier.com/locate/ijsolstr

Exact characteristic equations for some of classical boundary conditions of vibrating moderately thick rectangular plates

Shahrokh Hosseini Hashemi *, M. Arsanjani

School of Mechanical Engineering, Iran University of Science and Technology, Narmak, Tehran, Iran

Received 14 June 2004; received in revised form 17 June 2004
Available online 21 August 2004

Abstract

The dimensionless equations of motion are derived based on the Mindlin plate theory to study the transverse vibration of thick rectangular plates without further usage of any approximate method. The exact closed form characteristic equations are given within the validity of the Mindlin plate theory for plates having two opposite sides simply supported. The six distinct cases considered involve all possible combinations of classical boundary conditions at the other two sides of rectangular plates. Accurate eigenfrequency parameters are presented for a wide range of aspect ratio η and thickness ratio δ for each case. The three dimensional deformed mode shapes together with their associated contour plots obtained from the exact closed form eigenfunctions are also presented. Finally, the effect of boundary conditions, aspect ratios and thickness ratios on the eigenfrequency parameters and vibratory behavior of each distinct cases are studied in detail. It is believed that in the present work, the exact closed form characteristic equations and their associated eigenfunctions, except for the plates with four edges simply supported, for the rest of considered six cases are obtained for the first time.

Keywords: Mindlin plate; Vibration; Eigenfrequency; Eigenfunction; Rectangular; Mode shape; Closed form

* Corresponding author. Tel.: +9821 73912912; fax: +9821 7454050.
E-mail address: shh@iust.ac.ir (S.H. Hashemi).

0020-7683/$ - see front matter © 2004 Elsevier Ltd. All rights reserved.
doi:10.1016/j.ijsolstr.2004.06.063

1. Introduction

Rectangular plates are commonly used structural components in many branches of modern technology namely mechanical, aerospace, electronic, marine, optical, nuclear and structural engineering. Thus, the knowledge of their free vibrational behavior is very important to the structural designers.

The published work concerning vibration of such plates is abundant, however, the vast majority of it is based on thin plate theory. An excellent reference source may be found in the well-known work of Leissa (1969) and his subsequent articles (Leissa, 1977, 1978, 1981a,b, 1987a,b) published in Vibration Digest from time to time. His remarkable work on the free vibration of thin rectangular plates (Leissa, 1973) also present comprehensive and accurate analytical results for 21 distinct cases which involve all possible combinations of classical boundary conditions.

The thin plate theory neglects the effect of shear deformation and rotatory inertia which result in the over-estimation of vibration frequencies. This error increases with increasing plate thickness. Improving on the thin plate theory Mindlin and co-workers (Mindlin, 1951, 1956) proposed the so-called first-order shear deformation theory for moderately thick plates and incorporated the effect of rotatory inertia. The first-order shear deformation plate theory of Mindlin, however, requires a shear correction factor to compensate the error resulting from the approximation made on the nonuniform shear strain distribution.

Solutions of the eigenvalue problems of thick plates have been represented using several different approximate methods over the years. Dawe and Roufaeil (1980) treated the free vibration of Mindlin rectangular plates by the Rayliegh–Ritz method. They used the Timoshenko beam functions as the admissible functions of the plate. Liew et al. (1993a, 1995a) investigated the free vibration of Mindlin rectangular plates, respectively, by using two dimensional polynomials and one-dimensional Gram–Schmidt polynomials as the admissible functions of the plate in the Rayliegh–Ritz method. Cheung and Zhou (2000) developed a set of static Timoshenko beam functions as the admissible functions to study the vibration of moderately thick rectangular plates by the Rayliegh–Ritz method. The finite element, finite strip, finite layer, collocation and superposition methods have also been used, respectively, by Al Janabi et al. (1989); Dawe (1987); Cheung and Chakrabarti (1972); Mikami and Yoshimura (1984) and Gorman (1996) to study the eigenvalue problems of thick plates. Moreover, some investigations on three-dimensional vibrations of rectangular plates have been reported by Srinvas et al. (1970); Wittrick (1987); Liew et al. (1993b, 1994, 1995b); Liew and Teo (1999). More recently Zhou et al. (2002) investigated the free vibration of rectangular plates with any thickness using three-dimensional analysis and selecting the Chebyshev polynomials as the admissible functions of the plate in the Ritz method. A beneficial literature review on the vibration of thick rectangular plates have also been furnished by Liew and Xiang (1995). Other works of interest are Chen et al. (1997); Lim et al. (1998a,b); Malik and Bert (1998); Gorman (2000) and Liew et al. (1998).

The exact characteristic equations for rectangular thin plates having two opposite sides simply supported can be found in the original work of Leissa (1973). No such equations about thick plates are available in the literature. To fill this apparent void, the present work is carried out to provide the exact characteristic equations for the six cases having two opposite sides simply supported. The six cases considered are namely S–S–S–S, S–C–S–S, S–C–S–C, S–S–S–F, S–F–S–F and S–C–S–F plates. The integrated equations of motion in terms of the stress resultant are derived based on Mindlin plate theory for thick rectangular plates with consideration of transverse shear deformation and rotatory inertia. The frequency parameters calculated from the exact characteristic equations are extensively tabulated for all six cases, covering wide ranges of plate aspect ratios η and relative thickness ratio δ. These results may serve as benchmark solutions for validating approximate two-dimensional theories and new computational techniques in future. Three dimensional mode shapes and their associated contour plots for $\eta = 2$ and $\delta = 0.1$ are presented for each of the boundary conditions. The exact transverse deflections derived for each of the six cases also facilitate the study of forced vibration of Mindlin plates which will be dealt with in subsequent paper.

2. Governing equations and their dimensionless forms

Consider a thick rectangular plate of length a, width b, and uniform thickness h, oriented so that its undeformed middle surface contains the x_1 and x_2 axis of a Cartesian co-ordinate system (x_1,x_2,x_3), as shown in Fig. 1.

The displacements along the x_1 and x_2 axes are denoted by U_1 and U_2, respectively, while the displacement in the direction perpendicular to the undeformed middle surface is denoted by U_3. In the Mindlin plate theory, the displacement components are assumed to be given by

$$U_1 = -x_3\psi_1(x_1,x_2,t), \quad U_2 = -x_3\psi_2(x_1,x_2,t), \quad U_3 = \psi_3(x_1,x_2,t), \tag{1a,b,c}$$

where t is the time, ψ_3 is the transverse displacement, ψ_1 and ψ_2 are the slope due to bending alone in the respective planes. Using the displacement field given in Eq. ((1a)–(c)), the tensorial components of the strains may be expressed as

$$\varepsilon_{11} = -x_3\psi_{1,1}, \quad \varepsilon_{22} = -x_3\psi_{2,2}, \quad \varepsilon_{33} = 0, \tag{2a,b,c}$$

$$\varepsilon_{12} = -\tfrac{1}{2}(\psi_{1,2} + \psi_{2,1})x_3, \quad \varepsilon_{13} = -\tfrac{1}{2}(\psi_1 - \psi_{3,1}), \quad \varepsilon_{23} = -\tfrac{1}{2}(\psi_2 - \psi_{3,2}). \tag{2d,e,f}$$

Based on the strain–displacement relations given in Eq. (2) and assuming a stress distribution in accordance with Hook's law, as well as neglecting the stress–strain relations involving ε_{33} the resultant bending moments, twisting moments, and the transverse shear forces, all per unit length in terms of ψ_1, ψ_2 and ψ_3 are obtained by integrating the stresses and moment of the stresses through the thickness of the plate. These are given by

$$M_{11} = -D(\psi_{1,1} + v\psi_{2,2}), \quad M_{22} = -D(\psi_{2,2} + v\psi_{1,1}), \tag{3a,b}$$

$$M_{12} = -\frac{D}{2}(1-v)(\psi_{1,2} + \psi_{2,1}), \tag{3c}$$

$$Q_1 = -K^2Gh(\psi_1 - \psi_{3,1}), \quad Q_2 = -K^2Gh(\psi_2 - \psi_{3,2}), \tag{3d}$$

where v is the Poisson's ratio, $G = E/2(1+v)$ is the shear modulus, $D = Eh^3/12(1-v^2)$ is the flexural rigidity and K^2 is the shear correction factor to account for the fact that the transverse shear strains are not truly independent of the thickness coordinate.

The governing equations of motion may now be derived from the three-dimensional stress equations of motion which are written as

$$\sigma_{11,1} + \sigma_{12,2} + \sigma_{13,3} = \rho\ddot{U}_1, \quad \sigma_{21,1} + \sigma_{22,2} + \sigma_{23,3} = \rho\ddot{U}_2, \tag{4a,b}$$

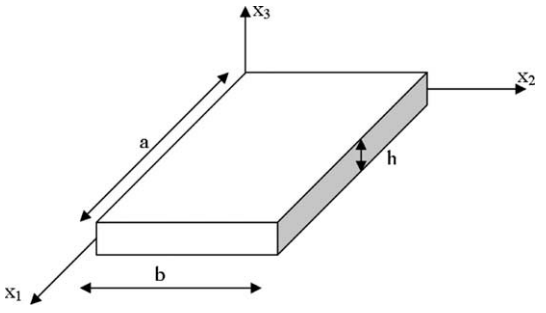

Fig. 1. A Mindlin plate with co-ordinate convention.

$$\sigma_{31,1} + \sigma_{32,2} + \sigma_{33,3} = \rho \ddot{U}_3, \tag{4c}$$

where ρ is the mass density per unit volume. The first two are multiplied by x_3 and then integrated through the thickness, making use of equations (3) and the fact that there are no shear forces applied to the faces of the plate, while the last equation is integrated through the thickness, making use of the fact that $\sigma_{33}|_{-h/2}^{h/2} = -q(x_1, x_2, t)$ is the applied load. Thus the integrated equations of motion in absence of the applied load and assumption of the free harmonic motion in terms of the stress resultants are given by

$$M_{11,1} + M_{12,2} - Q_1 = \frac{1}{12}\rho h^3 \omega^2 \psi_1, \quad M_{12,1} + M_{22,2} - Q_2 = \frac{1}{12}\rho h^3 \omega^2 \psi_2, \tag{5a,b}$$

$$Q_{1,1} + Q_{2,2} = -\rho h \omega^2 \psi_3. \tag{5c}$$

For generality and convenience, the coordinates are normalized with respect to the plate planar dimensions and the following nondimensional terms are introduced:

$$X_1 = \frac{x_1}{a}, \quad X_2 = \frac{x_2}{b}, \quad \delta = \frac{h}{a}, \quad \eta = \frac{a}{b}, \quad \beta = \omega a^2 \sqrt{\frac{\rho h}{D}}, \tag{6}$$

where β is the frequency parameter. The stress resultants may then be written in dimensionless form as

$$\widetilde{M}_{11} = -\left(\tilde{\psi}_{1,1} + v\eta\tilde{\psi}_{2,2}\right)e^{i\omega t} = \frac{M_{11}}{D}a, \quad \widetilde{M}_{22} = -\left(\eta\tilde{\psi}_{2,2} + v\tilde{\psi}_{1,1}\right)e^{i\omega t} = \frac{M_{22}}{D}a, \tag{7a,b}$$

$$\widetilde{M}_{12} = -v_1\left(\eta\tilde{\psi}_{1,2} + \tilde{\psi}_{2,1}\right)e^{i\omega t} = \frac{M_{12}}{D}a, \quad \left(v_1 = \frac{1-v}{2}\right) \tag{7c}$$

$$\widetilde{Q}_1 = -\left(\tilde{\psi}_1 - \tilde{\psi}_{3,1}\right)e^{i\omega t} = \frac{Q_1}{K^2 Gh}, \quad \widetilde{Q}_2 = -\left(\tilde{\psi}_2 - \eta\tilde{\psi}_{3,2}\right)e^{i\omega t} = \frac{Q_2}{K^2 Gh}, \tag{7d,e}$$

where comma-subscript convention represents the partial differentiation with respect to the normalized coordinates and

$$\tilde{\psi}_1(X_1, X_2) = \psi_1(x_1, x_2, t)e^{-i\omega t}, \quad \tilde{\psi}_2(X_1, X_2) = \psi_2(x_1, x_2, t)e^{-i\omega t}, \tag{8a, b}$$

$$\tilde{\psi}_3(X_1, X_2) = \psi_3(x_1, x_2, t)\frac{e^{-i\omega t}}{a}. \tag{8c}$$

Substitution of the dimensionless stress resultants from expressions (7a)–(7e) into Eqs. (5a)–(5c) leads to

$$\tilde{\psi}_{1,11} + \eta^2\tilde{\psi}_{1,22} + \frac{v_2}{v_1}\left(\tilde{\psi}_{1,11} + \eta\tilde{\psi}_{2,12}\right) - \frac{12K^2}{\delta^2}\left(\tilde{\psi}_1 - \tilde{\psi}_{3,1}\right) = -\frac{\beta^2\delta^2}{12v_1}\tilde{\psi}_1, \tag{9a}$$

$$\tilde{\psi}_{2,11} + \eta^2\tilde{\psi}_{2,22} + \frac{v_2}{v_1}\eta\left(\tilde{\psi}_{1,12} + \eta\tilde{\psi}_{2,22}\right) - \frac{12K^2}{\delta^2}\left(\tilde{\psi}_2 - \eta\tilde{\psi}_{3,2}\right) = -\frac{\beta^2\delta^2}{12v_1}\tilde{\psi}_2, \tag{9b}$$

$$\tilde{\psi}_{3,11} + \eta^2\tilde{\psi}_{3,22} - \left(\tilde{\psi}_{1,1} + \eta\tilde{\psi}_{2,2}\right) = -\frac{\beta^2\delta^2}{12K^2v_1}\tilde{\psi}_3, \tag{9c}$$

where $v_2 = (1 + v)/2$. The three dimensionless governing equations (9a)–(9c) may be solved by representing the three dimensionless functions $\tilde{\psi}_1$, $\tilde{\psi}_2$ and $\tilde{\psi}_3$ in terms of the three dimensionless potentials W_1, W_2 and W_3 as follow:

$$\tilde{\psi}_1 = C_1 W_{1,1} + C_2 W_{2,1} - \eta W_{3,2}, \quad \tilde{\psi}_2 = C_1\eta W_{1,2} + C_2\eta W_{2,2} + W_{3,1}, \tag{10a,b}$$

$$\tilde{\psi}_3 = W_1 + W_2, \tag{10c}$$

where

$$C_1 = 1 - \frac{\alpha_2^2}{\nu_1 \alpha_3^2}, \quad C_2 = 1 - \frac{\alpha_1^2}{\nu_1 \alpha_3^2}, \tag{11a,b}$$

$$\alpha_1^2, \alpha_2^2 = \frac{\beta^2}{2}\left[\frac{\delta^2}{12}\left(\frac{1}{K^2\nu_1}+1\right) \pm \sqrt{\left(\frac{\delta^2}{12}\right)^2\left(\frac{1}{K^2\nu_1}-1\right)^2 + \frac{4}{\beta^2}}\right], \tag{11c,d}$$

$$\alpha_3^2 = \frac{12K^2}{\beta^2\delta^2}\alpha_1^2\alpha_2^2 = \frac{12K^2}{\delta^2}\left(\frac{\beta^2\delta^4}{144K^2\nu_1} - 1\right). \tag{11e}$$

Based on these dimensionless potentials, the governing equations of motion may now be expressed as

$$W_{1,11} + \eta^2 W_{1,22} = -\alpha_1^2 W_1, \quad W_{2,11} + \eta^2 W_{2,22} = -\alpha_2^2 W_2, \tag{12a,b}$$

$$W_{3,11} + \eta^2 W_{3,22} = -\alpha_3^2 W_3. \tag{12c}$$

One set of solutions to Eqs. (12a)–(12c) are

$$W_1 = [A_1 \sin(\lambda_1 X_2) + A_2 \cos(\lambda_1 X_2)]\sin(\mu_1 X_1) + [B_1 \sin(\lambda_1 X_2) + B_2 \cos(\lambda_1 X_2)]\cos(\mu_1 X_1), \tag{13a}$$

$$W_2 = [A_3 \sinh(\lambda_2 X_2) + A_4 \cosh(\lambda_2 X_2)]\sin(\mu_2 X_1) + [B_3 \sinh(\lambda_2 X_2) + B_4 \cosh(\lambda_2 X_2)]\cos(\mu_2 X_1), \tag{13b}$$

$$W_3 = [A_5 \sinh(\lambda_3 X_2) + A_6 \cosh(\lambda_3 X_2)]\cos(\mu_3 X_1) + [B_5 \sinh(\lambda_3 X_2) + B_6 \cosh(\lambda_3 X_2)]\sin(\mu_3 X_1), \tag{13c}$$

where A_i and B_i are the arbitrary constants. λ_i and μ_i are also related to the α_i by

$$\alpha_1^2 = \mu_1^2 + \eta^2\lambda_1^2, \quad \alpha_2^2 = \mu_2^2 - \eta^2\lambda_2^2, \quad \alpha_3^2 = \mu_3^2 - \eta^2\lambda_3^2. \tag{14a,b,c}$$

The details of existence of the other sets of solutions are given in Appendix A. It should be emphasized that, as shown in Appendix A the set of solutions given by Eqs. (13a)–(13c) are based on the assumption that

$$\alpha_1^2 > 0, \quad \alpha_2^2 < 0, \quad \alpha_3^2 < 0. \tag{15}$$

3. Two opposite edges simply-supported

For the sake of definiteness, the dimensionless boundary conditions will be given below for an edge parallel to the X_2-normalized axis (for example, the boundaries $X_1 = 0$ or $X_1 = 1$). For a simply-supported edge

$$\widetilde{M}_{11} = \tilde{\psi}_2 = \tilde{\psi}_3 = 0 \tag{16a}$$

for a free edge

$$\widetilde{M}_{11} = \widetilde{M}_{12} = \widetilde{Q}_1 = 0 \tag{16b}$$

and for a clamped edge

$$\tilde{\psi}_1 = \tilde{\psi}_2 = \tilde{\psi}_3 = 0. \tag{16c}$$

Corresponding boundary conditions for the edges $X_2 = 0$ and $X_2 = 1$ are obtained by interchanging subscripts 1 and 2 in Eqs. (16a)–(16c).

On the assumption of a simply-supported edge at both $X_1 = 0$ and $X_1 = 1$, Eqs. (13a)–(13c) may be written as

$$W_1 = [A_1 \sin(\lambda_1 X_2) + A_2 \cos(\lambda_1 X_2)] \sin(m\pi X_1), \tag{17a}$$

$$W_2 = [A_3 \sinh(\lambda_2 X_2) + A_4 \cosh(\lambda_2 X_2)] \sin(m\pi X_1), \tag{17b}$$

$$W_3 = [A_5 \sinh(\lambda_3 X_2) + A_6 \cosh(\lambda_3 X_2)] \cos(m\pi X_1), \tag{17c}$$

where $m = 1,2,\ldots$. Introducing Eqs. (17a)–(17c) in Eqs. (10a)–(10c) and substituting the results into the three appropriate boundary conditions along the edges $X_2 = 0$ and $X_2 = 1$ lead to a characteristic determinant of the six order for each m. Expanding the determinant and collecting terms yields a characteristic equation. The characteristic equations for the six cases are listed below.

Case 1. S–S–S–S

$$\sin\lambda_1 \sinh\lambda_2 \sinh\lambda_3 = 0. \tag{18}$$

Case 2. S–C–S–S

$$(C_1 - C_2)\mu^2 \tan\lambda_1 \tanh\lambda_2 - \eta^2\lambda_3(C_1\lambda_1 \tanh\lambda_2 - C_2\lambda_2 \tan\lambda_1)\tanh\lambda_3 = 0. \tag{19}$$

Case 3. S–C–S–C

$$\begin{aligned} &2(C_1 - C_2)\eta^2\mu^2\lambda_3[C_2\lambda_2(\cosh\lambda_2\cosh\lambda_3 - 1)\sin\lambda_1 - C_1\lambda_1(\cos\lambda_1\cosh\lambda_3 - 1)\sinh\lambda_2] \\ &\quad + \left[(C_1 - C_2)^2\mu^4 + \left(C_2^2\lambda_2^2 - C_1^2\lambda_1^2\right)\eta^4\lambda_3^2\right]\sin\lambda_1\sinh\lambda_2\sinh\lambda_3 \\ &\quad - 2C_1C_2\eta^4\lambda_3^2\lambda_1\lambda_2(\cos\lambda_1\cosh\lambda_2 - 1)\sinh\lambda_3 = 0. \end{aligned} \tag{20}$$

Case 4. S–S–S–F

$$C_2\lambda_1L_1L_2\tanh\lambda_2 + C_1\lambda_2L_3L_4\tan\lambda_1 - 2(C_1 - C_2)\eta^2\mu^2\lambda_1\lambda_2\lambda_3(1 - \nu)\tanh\lambda_3 = 0, \tag{21}$$

where

$$\begin{aligned} &L_1 = (C_1 - 1)\eta^2\lambda_3^2 - (C_1 + 1)\mu^2, \quad L_2 = \eta^2\lambda_2^2 - \nu\mu^2, \\ &L_3 = (C_2 - 1)\eta^2\lambda_3^2 - (C_2 + 1)\mu^2, \quad L_4 = \eta^2\lambda_1^2 + \nu\mu^2. \end{aligned} \tag{22a,b,c,d}$$

Case 5. S–F–S–F

$$\begin{aligned} &4(C_1 - C_2)\eta^2\mu^2\lambda_1\lambda_2\lambda_3[C_1\lambda_2L_3L_4(\cos\lambda_1\cosh\lambda_3 - 1)\sinh\lambda_2 - C_2\lambda_1L_1L_2(\cosh\lambda_2\cosh\lambda_3 - 1)\sin\lambda_1](1 - \nu) \\ &\quad + \left[4(C_1 - C_2)^2\eta^4\mu^4\lambda_1^2\lambda_2^2\lambda_3^2(1 - \nu)^2 + C_2^2\lambda_1^2L_1^2L_2^2 - C_1^2\lambda_2^2L_3^2L_4^2\right]\sin\lambda_1\sinh\lambda_2\sinh\lambda_3 \\ &\quad - 2C_1C_2\lambda_1\lambda_2L_1L_2L_3L_4(\cos\lambda_1\cosh\lambda_2 - 1)\sinh\lambda_3 = 0. \end{aligned} \tag{23}$$

Case 6. S–C–S–F

$$\begin{aligned} &\lambda_1\lambda_2\lambda_3\eta^2\left[C_2^2L_1L_2 - C_1^2L_3L_4 - 2(C_1 - C_2)^2\mu^4(1 - \nu)\right]\cos\lambda_1\cosh\lambda_2\cosh\lambda_3 \\ &\quad + (C_1 - C_2)C_2\lambda_1\mu^2\left\{\left[L_1L_2 - 2(1 - \nu)\lambda_2^2\lambda_3^2\eta^4\right]\sinh\lambda_2\sinh\lambda_3\right. \\ &\quad \left.+\lambda_2\lambda_3\eta^2[L_1(1 - \nu) - 2L_2]\right\}\cos\lambda_1 + (C_1 - C_2)C_1\lambda_2\mu^2\left\{\left[L_3L_4 - 2(1 - \nu)\lambda_1^2\lambda_3^2\eta^4\right]\sin\lambda_1\sinh\lambda_3\right. \\ &\quad \left.-\lambda_1\lambda_3\eta^2[L_3(1 - \nu) + 2L_4]\right\}\cosh\lambda_2 + C_1C_2\lambda_3\eta^2\left[\left(L_1L_2\lambda_1^2 + L_3L_4\lambda_2^2\right)\sin\lambda_1\sinh\lambda_2\right. \\ &\quad \left.+\lambda_1\lambda_2(L_1L_4 - L_2L_3)\right]\cosh\lambda_3 = 0. \end{aligned} \tag{24}$$

In Eqs. (18)–(24)

$$\mu = m\pi, \tag{25a}$$

and λ_1,λ_2 and λ_3 are related to nondimensional frequency parameter through relations

$$\lambda_1 = \frac{1}{\eta}\sqrt{\alpha_1^2 - m^2\pi^2}, \quad \lambda_2 = \frac{1}{\eta}\sqrt{-\alpha_2^2 + m^2\pi^2}, \quad \lambda_3 = \frac{1}{\eta}\sqrt{-\alpha_3^2 + m^2\pi^2}. \tag{25b,c,d}$$

A point frequently overlooked in the literature is that it is possible for α_1^2 to be less than $m^2\pi^2$. When this occur it is necessary to replace $\sin(\lambda_1 X_2)$ and $\cos(\lambda_1 X_2)$ in Eq. (17a) by $\sinh(\tilde{\lambda}_1 X_2)$ and $\cosh(\tilde{\lambda}_1 X_2)$, respectively, where

$$\tilde{\lambda}_1 = \frac{1}{\eta}\sqrt{-\alpha_1^2 + m^2\pi^2}. \tag{26}$$

Thus the characteristic equations become the following.

Case 1. S–S–S–S

$$\sinh\tilde{\lambda}_1 \sinh\lambda_2 \sinh\lambda_3 = 0. \tag{27}$$

Case 2. S–C–S–S

$$(C_1 - C_2)\mu^2 \tanh\tilde{\lambda}_1 \tanh\lambda_2 - \eta^2\lambda_3\left(C_1\tilde{\lambda}_1 \tanh\lambda_2 - C_2\lambda_2 \tanh\tilde{\lambda}_1\right)\tanh\lambda_3 = 0. \tag{28}$$

Case 3. S–C–S–C

$$\begin{aligned} &2(C_1 - C_2)\eta^2\mu^2\lambda_3\left[C_2\lambda_2(\cosh\lambda_2\cosh\lambda_3 - 1)\sinh\tilde{\lambda}_1 - C_1\tilde{\lambda}_1\left(\cosh\tilde{\lambda}_1\cosh\lambda_3 - 1\right)\sinh\lambda_2\right] \\ &\quad + \left[(C_1 - C_2)^2\mu^4 + \left(C_2^2\lambda_2^2 + C_1^2\tilde{\lambda}_1^2\right)\eta^4\lambda_3^2\right]\sinh\tilde{\lambda}_1\sinh\lambda_2\sinh\lambda_3 \\ &\quad - 2C_1C_2\eta^4\lambda_3^2\tilde{\lambda}_1\lambda_2\left(\cosh\tilde{\lambda}_1\cosh\lambda_2 - 1\right)\sinh\lambda_3 = 0. \end{aligned} \tag{29}$$

Case 4. S–S–S–F

$$C_2\tilde{\lambda}_1 L_1 L_2 \tanh\lambda_2 + C_1\lambda_2 L_3\tilde{L}_4 \tanh\tilde{\lambda}_1 - 2(C_1 - C_2)\eta^2\mu^2\tilde{\lambda}_1\lambda_2\lambda_3(1 - \nu)\tanh\lambda_3 = 0. \tag{30}$$

where

$$\tilde{L}_4 = -\eta^2\tilde{\lambda}_1^2 + \nu\mu^2. \tag{31}$$

Case 5. S–F–S–F

$$\begin{aligned} &4(C_1 - C_2)\eta^2\mu^2\tilde{\lambda}_1\lambda_2\lambda_3\left[C_1\lambda_2 L_3\tilde{L}_4\left(\cosh\tilde{\lambda}_1\cosh\lambda_3 - 1\right)\sinh\lambda_2\right. \\ &\quad \left. + C_2\tilde{\lambda}_1 L_1 L_2(\cosh\lambda_2\cosh\lambda_3 - 1)\sinh\tilde{\lambda}_1\right](1 - \nu) \\ &\quad - \left[4(C_1 - C_2)^2\eta^4\mu^4\tilde{\lambda}_1^2\lambda_2^2\lambda_3^2(1 - \nu)^2 + C_2^2\tilde{\lambda}_1^2 L_1^2 L_2^2 + C_1^2\lambda_2^2 L_3^2\tilde{L}_4^2\right]\sinh\tilde{\lambda}_1\sinh\lambda_2\sinh\lambda_3 \\ &\quad - 2C_1C_2\tilde{\lambda}_1\lambda_2 L_1 L_2 L_3\tilde{L}_4\left(\cosh\tilde{\lambda}_1\cosh\lambda_2 - 1\right)\sinh\lambda_3 = 0. \end{aligned} \tag{32}$$

Case 6. S–C–S–F

$$\begin{aligned}
&\tilde{\lambda}_1\lambda_2\lambda_3\eta^2\left[C_2^2L_1L_2 - C_1^2L_3\widetilde{L}_4 - 2(C_1-C_2)^2\mu^4(1-\nu)\right]\cosh\tilde{\lambda}_1\cosh\lambda_2\cosh\lambda_3\\
&+(C_1-C_2)C_2\tilde{\lambda}_1\mu^2\left\{\left[L_1L_2 - 2(1-\nu)\lambda_2^2\lambda_3^2\eta^4\right]\sinh\lambda_2\sinh\lambda_3 + \lambda_2\lambda_3\eta^2[L_1(1-\nu)-2L_2]\right\}\cosh\tilde{\lambda}_1\\
&+(C_1-C_2)C_1\lambda_2\mu^2\left\{\left[L_3\widetilde{L}_4 + 2(1-\nu)\tilde{\lambda}_1^2\lambda_3^2\eta^4\right]\sinh\tilde{\lambda}_1\sinh\lambda_3 - \tilde{\lambda}_1\lambda_3\eta^2\left[L_3(1-\nu)+2\widetilde{L}_4\right]\right\}\cosh\lambda_2\\
&-C_1C_2\lambda_3\eta^2\left[\left(L_1L_2\tilde{\lambda}_1^2 - L_3\widetilde{L}_4\lambda_2^2\right)\sinh\tilde{\lambda}_1\sinh\lambda_2 - \tilde{\lambda}_1\lambda_2\left(L_1\widetilde{L}_4 - L_2L_3\right)\right]\cosh\lambda_3 = 0.
\end{aligned} \tag{33}$$

Because of the geometric symmetry which exists about the axis $x_2 = b/2$ (i.e., "x_2-symmetry") in case 1, 3 and 5, vibration modes in these cases will separate into ones which are either x_2-symmetric or x_2-antisymmetric. The characteristic equations corresponding to those modes can be obtained from Eqs. (18), (20), (23), (27), (29) and (32) by factoring, or by new derivations in terms of a coordinate system having its origin in the centre of the plate. The resulting equations are the following.

Case 1. S–S–S–S

$$\alpha_1^2 > m^2\pi^2 \quad \begin{cases} \text{symmetric}: & \cos\dfrac{\lambda_1}{2}\cosh\dfrac{\lambda_2}{2}\cosh\dfrac{\lambda_3}{2} = 0,\\[2ex] \text{antisymmetric}: & \sin\dfrac{\lambda_1}{2}\sinh\dfrac{\lambda_2}{2}\sinh\dfrac{\lambda_3}{2} = 0, \end{cases} \tag{34a,b}$$

$$\alpha_1^2 < m^2\pi^2 \quad \begin{cases} \text{symmetric}: & \cosh\dfrac{\tilde{\lambda}_1}{2}\cosh\dfrac{\lambda_2}{2}\cosh\dfrac{\lambda_3}{2} = 0,\\[2ex] \text{antisymmetric}: & \sinh\dfrac{\tilde{\lambda}_1}{2}\sinh\dfrac{\lambda_2}{2}\sinh\dfrac{\lambda_3}{2} = 0. \end{cases} \tag{34c,d}$$

Case 3. S–C–S–C

$$\alpha_1^2 > m^2\pi^2 \quad \begin{cases} \text{symmetric}: & \lambda_3\eta^2\left(C_2\lambda_2\tanh\dfrac{\lambda_2}{2} + C_1\lambda_1\tan\dfrac{\lambda_1}{2}\right) + (C_1-C_2)\mu^2\tanh\dfrac{\lambda_3}{2} = 0,\\[2ex] \text{antisymmetric}: & \lambda_3\eta^2\left(C_2\lambda_2\tan\dfrac{\lambda_1}{2} - C_1\lambda_1\tanh\dfrac{\lambda_2}{2}\right)\tanh\dfrac{\lambda_3}{2} + (C_1-C_2)\mu^2\tan\dfrac{\lambda_1}{2}\tanh\dfrac{\lambda_2}{2} = 0, \end{cases} \tag{35a,b}$$

$$\alpha_1^2 < m^2\pi^2 \quad \begin{cases} \text{symmetric}: & \lambda_3\eta^2\left(C_2\lambda_2\tanh\dfrac{\lambda_2}{2} - C_1\tilde{\lambda}_1\tanh\dfrac{\tilde{\lambda}_1}{2}\right) + (C_1-C_2)\mu^2\tanh\dfrac{\lambda_3}{2} = 0,\\[2ex] \text{antisymmetric}: & \lambda_3\eta^2\left(C_2\lambda_2\tanh\dfrac{\tilde{\lambda}_1}{2} - C_1\tilde{\lambda}_1\tanh\dfrac{\lambda_2}{2}\right)\tanh\dfrac{\lambda_3}{2} + (C_1-C_2)\mu^2\tanh\dfrac{\tilde{\lambda}_1}{2}\tanh\dfrac{\lambda_2}{2} = 0. \end{cases} \tag{35c,d}$$

Case 5. S–F–S–F

$$\alpha_1^2 > m^2\pi^2 \begin{cases} \text{symmetric}: & \left(C_2\lambda_1 L_1 L_2 \tan\dfrac{\lambda_1}{2} - C_1\lambda_2 L_3 L_4 \tanh\dfrac{\lambda_2}{2}\right)\tanh\dfrac{\lambda_3}{2} \\ & -2(C_1 - C_2)\eta^2\lambda_1\lambda_2\lambda_3\mu^2(1-\nu)\tan\dfrac{\lambda_1}{2}\tanh\dfrac{\lambda_2}{2} = 0, \\ \text{antisymmetric}: & C_1\lambda_2 L_3 L_4 \tan\dfrac{\lambda_1}{2} + C_2\lambda_1 L_1 L_2 \tanh\dfrac{\lambda_2}{2} \\ & -2(C_1 - C_2)\eta^2\lambda_1\lambda_2\lambda_3\mu^2(1-\nu)\tanh\dfrac{\lambda_3}{2} = 0, \end{cases} \tag{36a,b}$$

$$\alpha_1^2 < m^2\pi^2 \begin{cases} \text{symmetric}: & \left(C_2\tilde{\lambda}_1 L_1 L_2 \tanh\dfrac{\tilde{\lambda}_1}{2} + C_1\lambda_2 L_3 \widetilde{L}_4 \tanh\dfrac{\lambda_2}{2}\right)\tanh\dfrac{\lambda_3}{2} \\ & -2(C_1 - C_2)\eta^2\tilde{\lambda}_1\lambda_2\lambda_3\mu^2(1-\nu)\tanh\dfrac{\tilde{\lambda}_1}{2}\tanh\dfrac{\lambda_2}{2} = 0, \\ \text{antisymmetric}: & C_1\lambda_2 L_3 \widetilde{L}_4 \tanh\frac{\tilde{\lambda}_1}{2} + C_2\tilde{\lambda}_1 L_1 L_2 \tanh\dfrac{\lambda_2}{2} \\ & -2(C_1 - C_2)\eta^2\tilde{\lambda}_1\lambda_2\lambda_3\mu^2(1-\nu)\tanh\dfrac{\lambda_3}{2} = 0. \end{cases} \tag{36c,d}$$

It is also seen that, for example, Eqs. (35b) and (35d) are the same as Eqs. (19) and (28), respectively, except that λ_1, λ_2 and λ_3 have been replaced by $\lambda_1/2$, $\lambda_2/2$ and $\lambda_3/2$, respectively. The physical significance of this is that the x_2-antisymmetric modes of vibration (and the corresponding frequencies) of an S–C–S–C plate of length to width ratio η are the same as those of an S–C–S–S plate of length to width ratio 2η. This is because the conditions along the antisymmetric axis of an S–C–S–C plate are the same as conditions of a simple support. The same corresponding exists between Eqs. (36b) and (36d) for the S–F–S–F plate and Eqs. (21) and (30) for the S–S–S–F plate.

In order to find the nondimensional transverse deflection, previously mentioned procedure in determination of the characteristic equation for the six cases may be applied. Focusing on arbitrary constants A_i and presenting them in terms of A_1, leads to the following nondimensional transverse displacements for each cases.

Case 1. S–S–S–S

$$\widetilde{U}_3 = A_1 \sin(\lambda_1 X_2)\sin(m\pi X_1). \tag{37}$$

Case 2. S–C–S–S

$$\widetilde{U}_3 = A_1\left[\sin(\lambda_1 X_2) - \frac{\sin\lambda_1}{\sinh\lambda_2}\sinh(\lambda_2 X_2)\right]\sin(m\pi X_1). \tag{38}$$

Case 3. S–C–S–C

$$\widetilde{U}_3 = A_1\left[\sin(\lambda_1 X_2) + b_1\cos(\lambda_1 X_2) - (b_1\cos\lambda_1 - b_1\cosh\lambda_2 + \sin\lambda_1)\frac{\sinh(\lambda_2 X_2)}{\sinh\lambda_2} - b_1\cosh(\lambda_2 X_2)\right]\sin(m\pi X_1), \tag{39}$$

where

$$b_1 = -\frac{\eta^2\lambda_3(C_2\lambda_2\sin\lambda_1 - C_1\lambda_1\sinh\lambda_2)\sinh\lambda_3 + (C_1 - C_2)\mu^2\sin\lambda_1\sinh\lambda_2}{C_2\eta^2\lambda_2\lambda_3(\cos\lambda_1 - \cosh\lambda_2)\sinh\lambda_3 + (C_1 - C_2)\mu^2(\cos\lambda_1 - \cosh\lambda_3)\sinh\lambda_2}. \tag{40}$$

Case 4. S–S–S–F

$$\widetilde{U}_3 = A_1\left\{[\sin(\lambda_1 X_2) + b_2\cos(\lambda_1 X_2)]\cosh\lambda_2 + \frac{L_1\lambda_1}{L_3\lambda_2}\sinh[\lambda_2(1 - X_2)] - (b_2\cos\lambda_1 + \sin\lambda_1)\cosh(\lambda_2 X_2)\right\} \times \frac{\sin(m\pi X_1)}{\cosh\lambda_2}, \tag{41}$$

where

$$b_2 = -\frac{R_1}{R_2}, \tag{42a}$$

$$R_1 = C_2L_2(L_3\lambda_2\sin\lambda_1 - L_1\lambda_1\sinh\lambda_2)\cosh\lambda_3 + (C_1 - C_2)\lambda_2\mu^2(1 - \nu)(L_3\sin\lambda_1 + 2\eta^2\lambda_1\lambda_3\sinh\lambda_3)\cosh\lambda_2, \tag{42b}$$

$$R_2 = L_3\lambda_2\{C_2L_2\cos\lambda_1\cosh\lambda_3 + [(C_1 - C_2)\mu^2(1 - \nu)\cos\lambda_1 + C_1L_4\cosh\lambda_3]\cosh\lambda_2\}. \tag{42c}$$

Case 5. S–F–S–F

$$\widetilde{U}_3 = A_1\left[\sin(\lambda_1 X_2) + b_3\cos(\lambda_1 X_2) - \frac{L_1\lambda_1}{L_3\lambda_2}\sinh(\lambda_2 X_2) + b_4\cosh(\lambda_2 X_2)\right]\sin(m\pi X_1), \tag{43}$$

where

$$b_3 = -\frac{R_3}{R_4}, \quad b_4 = \frac{R_5}{R_6}, \tag{44a,b}$$

$$R_3 = 2(C_1 - C_2)\eta^2\mu^2\lambda_1\lambda_2\lambda_3(1 - \nu)(\cos\lambda_1 - \cosh\lambda_3)\sinh\lambda_2 - C_2L_1L_2\lambda_1(\cos\lambda_1 - \cosh\lambda_2)\sinh\lambda_3, \tag{44c}$$

$$R_4 = C_2L_1L_2\lambda_1\sin\lambda_1\sinh\lambda_3 - \lambda_2[2(C_1 - C_2)\eta^2\mu^2\lambda_1\lambda_3(1 - \nu)\sin\lambda_1 + C_1L_3L_4\sinh\lambda_3]\sinh\lambda_2, \tag{44d}$$

$$R_5 = \eta^2\lambda_1\lambda_3(1 - \nu)[(C_2 - 1)L_1(\cosh\lambda_2 - \cosh\lambda_3) + (C_1 - 1)L_3(b_3\sin\lambda_1 - \cos\lambda_1 + \cosh\lambda_3)] - b_3C_1L_3L_4\sinh\lambda_3, \tag{44e}$$

$$R_6 = L_3[(C_2 - 1)\eta^2\lambda_2\lambda_3(1 - \nu)\sinh\lambda_2 - C_2L_2\sinh\lambda_3]. \tag{44f}$$

Case 6. S–C–S–F

$$\widetilde{U}_3 = A_1\left\{[\sin(\lambda_1 X_2) + b_5\cos(\lambda_1 X_2)]\cosh\lambda_2 + \frac{L_1\lambda_1}{L_3\lambda_2}\sinh[\lambda_2(1 - X_2)] - (b_5\cos\lambda_1 + \sin\lambda_1)\cosh(\lambda_2 X_2)\right\} \times \frac{\sin(m\pi X_1)}{\cosh\lambda_2}, \tag{45}$$

where

$$b_5 = -\frac{R_7}{R_8}, \tag{46a}$$

$$R_7 = C_2L_2(L_3\lambda_2 \sin\lambda_1 - L_1\lambda_1 \sinh\lambda_2)\cosh\lambda_3 + (C_1 - C_2)\mu^2\lambda_2(1-\nu)(L_3 \sin\lambda_1 + 2\eta^2\lambda_1\lambda_3 \sinh\lambda_3)\cosh\lambda_2, \tag{46b}$$

$$R_8 = L_3\lambda_2[(C_1 - C_2)\mu^2(1-\nu)\cos\lambda_1 \cosh\lambda_2 + (C_2L_2 \cos\lambda_1 + C_1L_4 \cosh\lambda_2)\cosh\lambda_3]. \tag{46c}$$

4. Results and discussion

The eigenvalues obtained from the exact characteristic equations presented in Section 3 have been expressed in terms of the nondimensional frequency parameter $\beta = \omega a^2\sqrt{\rho h/D}$ where the symbols are as defined in Section 2. Numerical calculations have been performed for each of the six cases with arrangement of the boundary conditions as shown in Fig. 2. For the analysis, Poisson's ratio $\nu = 0.3$ and shear correction factor $K^2 = 0.86667$ have been used. The results are given in Tables 1–6 for the thickness to length ratios $\delta = 0.01$, 0.05, 0.1, 0.15 and 0.2 over a range of a aspect ratios $\eta = 0.4$, 0.5, 2/3, 1, 1.5, 2 and 2.5.

In each table, for each values of η and δ, the nine lowest values of β are displayed in increasing sequence. The results are exhibited in considerable accuracy simply because they were easily obtained to the accuracy given, and because they may be of worth to someone desiring to investigate the accuracy of an approximate method on some of these problems.

In addition, for each eigenvalue presented, the corresponding mode shape is described by the number of half waves in each direction. Thus for example, a 42-mode has four half waves in the x_1-direction and two in the x_2-direction. As an illustration a typical three dimensional deformed mode shapes together with their corresponding deflection counter plots for plate with aspect ratio $\eta = 2$ and thickness ratio $\delta = 0.1$ are given in Figs. 3–8. These figures express vividly the vibratory motion of the plate in each mode, for all considered six different boundary conditions. To compute the three dimensional deformed mode shapes, the exact transverse displacements given in Section 3 are used.

For all six cases the wave forms are, of course, sine functions in the x_1-direction, according to their corresponding equations of transverse displacement. Furthermore, the wave forms in the x_2-direction are sine function exactly for the S–S–S–S case only, whereas for the other cases the forms are only approximately

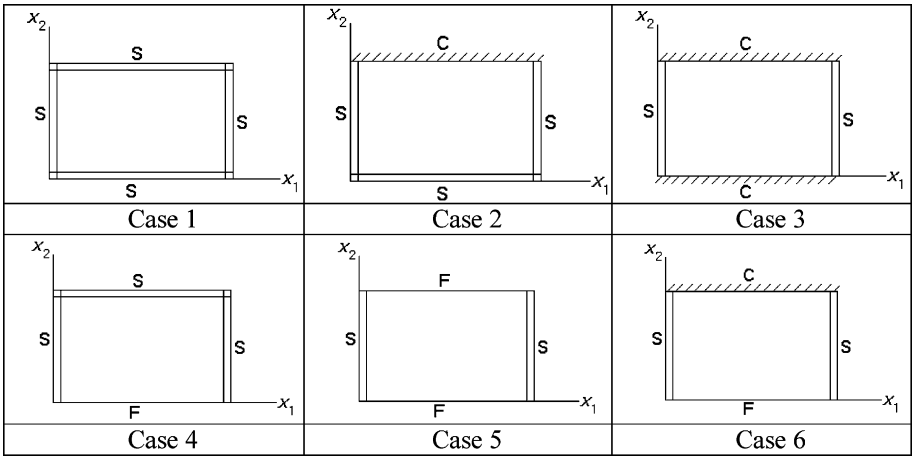

Fig. 2. Boundary conditions of Mindlin plates analaysed.

Table 1
First nine frequency parameters, $\beta = \omega a^2 \sqrt{\rho h/D}$, for rectangular Mindlin plates: Case 1 (S–S–S–S)

η	δ	1		2		3		4		5		6		7		8		9	
0.4	0.01	11.4464	11	16.1815	12	24.0715	13	35.1137	14	41.0274	21	45.7575	22	49.3045	15	53.6391	23	64.6697	24
	0.05	11.3906	11	16.0704	12	23.8273	13	34.5988	14	40.3278	21	44.8905	22	48.3006	15	52.4550	23	62.9631	24
	0.1	11.226	11	15.7408	12	23.1193	13	33.1515	14	38.3928	21	42.5226	22	45.5845	15	49.2869	23	58.5216	24
	0.15	10.9617	11	15.2421	12	22.0911	13	31.1557	14	35.7913	21	39.4002	22	42.0625	15	45.2344	23	53.0591	24
	0.2	10.6307	11	14.6304	12	20.8901	13	28.9548	14	32.9979	21	36.1126	22	38.3847	15	41.0929	23	47.6782	24
0.5	0.01	12.3343	11	19.7322	12	32.0578	13	41.9144	21	49.3045	22	49.3045	14	61.6170	23	71.4632	15	78.8455	24
	0.05	12.2696	11	19.5676	12	31.6276	13	41.1847	21	48.3006	14	48.3006	22	60.0641	23	69.3900	15	76.3360	24
	0.1	12.0752	11	19.0840	12	30.4080	13	39.1713	21	45.5845	14	45.5845	22	55.9920	23	64.0823	15	70.0219	24
	0.15	11.7747	11	18.3661	12	28.7028	13	36.4745	21	42.0525	22	42.0525	14	50.9309	23	57.7001	15	62.6035	24
	0.2	11.3961	11	17.5055	12	26.7944	13	33.5896	21	38.3847	14	38.3847	22	45.8969	23	51.5392	15	55.5860	24
2/3	0.01	14.2525	11	27.4021	12	43.8305	21	49.3045	13	56.9663	22	78.8455	23	79.9390	14	93.0579	31	106.1706	32
	0.05	14.1662	11	27.0866	12	43.0338	21	48.3006	13	55.6341	22	76.3360	23	77.3616	14	89.5992	31	101.7120	32
	0.1	13.9085	11	26.1803	12	40.8467	21	45.5846	13	52.1001	22	70.0219	23	70.8929	14	81.1723	31	91.1515	32
	0.15	13.5147	11	24.8863	12	37.9402	21	42.0525	13	47.6345	22	62.6035	23	63.3181	14	71.6723	31	79.6527	32
	0.2	13.0250	11	23.4005	12	34.8558	21	38.3847	13	43.1236	22	55.5860	23	56.1731	14	62.9921	31	69.4356	32
1	0.01	19.7322	11	49.3045	12	49.3045	21	78.8455	22	98.5222	13	98.5222	31	128.0114	23	128.0114	32	167.2821	14
	0.05	19.5676	11	48.3006	12	48.3006	21	76.3360	22	94.6612	13	94.6612	31	121.6319	23	121.6319	32	156.6852	14
	0.1	19.0840	11	45.5845	12	45.5845	21	70.0219	22	85.3654	13	85.3654	31	107.1775	23	107.1775	32	134.3586	14
	0.15	18.3661	11	42.0525	12	42.0525	21	62.6035	22	75.0402	13	75.0402	31	92.2350	23	92.2350	32	113.0257	14
	0.2	17.5055	11	38.3847	12	38.3847	21	55.5860	22	65.7193	13	65.7193	31	79.4758	23	79.4758	32	95.8088	14
1.5	0.01	32.0578	11	61.6170	21	98.5222	12	110.8131	31	128.0114	22	177.0912	32	179.5429	41	208.9471	13	238.3205	23
	0.05	31.6276	11	60.0641	21	94.6612	12	105.9727	31	121.6319	22	165.2949	32	167.4381	41	192.8740	13	217.8092	23
	0.1	30.4080	11	55.9920	21	85.3654	12	94.6182	31	107.1775	22	140.8579	32	142.4658	41	161.2626	13	179.2185	23
	0.15	28.7028	11	50.9309	21	75.0402	12	82.3977	31	92.2350	22	117.9100	32	119.1136	41	133.0590	13	146.1853	23
	0.2	26.7944	11	45.8969	21	65.7193	12	71.6377	31	79.4758	22	99.6076	32	100.5418	41	111.3137	13	121.3768	23
2	0.01	49.3045	11	78.8455	21	128.0114	31	167.2821	12	196.6991	22	196.6991	41	245.6590	32	284.7657	51	314.0601	42
	0.05	48.3006	11	76.3360	21	121.6319	31	156.6852	12	182.3382	22	182.3382	41	223.9679	32	256.3294	51	280.0876	42
	0.1	45.5845	11	70.0219	21	107.1775	31	134.3586	12	153.5390	22	153.5390	41	183.5877	32	206.1567	51	222.3439	42
	0.15	42.0525	11	62.6035	21	92.2350	31	113.0257	12	127.3559	22	127.3559	41	149.3536	32	165.5766	51	177.0802	42
	0.2	38.3847	11	55.5860	21	79.4758	31	95.8088	12	106.9195	22	106.9195	41	123.7961	32	136.1329	51	144.8367	42
2.5	0.01	71.4632	11	100.9808	21	150.1079	31	218.7416	41	255.4408	12	284.7657	22	306.7394	51	333.5728	32	401.7611	42
	0.05	69.3900	11	96.9321	21	141.4725	31	201.2400	41	232.1341	12	256.3294	22	274.1879	51	295.6941	32	348.9431	42
	0.1	64.0824	11	87.2358	21	122.7104	31	167.3362	41	189.3433	12	206.1567	22	218.3524	51	232.8175	32	267.7055	42
	0.15	57.7001	11	76.5366	21	104.1921	31	137.5189	41	153.5129	12	165.5766	22	174.2530	51	184.4713	32	208.8358	42
	0.2	51.5392	11	66.9264	21	88.9037	31	114.7404	41	126.9669	12	136.1329	22	142.6999	51	150.4103	32	168.7084	42

Table 2
First nine frequency parameters, $\beta = \omega a^2 \sqrt{\rho h/D}$, for rectangular Mindlin plates: Case 2 (S–C–S–S)

η	δ	1		2		3		4		5		6		7		8		9	
0.4	0.01	11.7476	11	17.1812	12	25.9035	13	37.8029	14	41.1764	21	46.3224	22	52.8453	15	54.8155	23	66.5794	24
	0.05	11.6850	11	17.0406	12	25.5844	13	37.1372	14	40.4657	21	45.4099	22	51.5765	15	53.5247	23	64.6733	24
	0.1	11.4978	11	16.6289	12	24.6755	13	35.3040	14	38.5047	21	42.9370	22	48.2205	15	50.1169	23	59.8000	24
	0.15	11.2099	11	16.0131	12	23.3910	13	32.8522	14	35.8757	21	33.7062	22	43.9968	15	45.8272	23	53.9333	24
	0.2	10.8485	11	15.2883	12	21.9343	13	30.2342	14	33.0596	21	36.3314	22	39.7527	15	41.5028	23	48.2574	24
0.5	0.01	12.9152	11	21.5239	12	35.1857	13	42.2071	21	50.3833	22	53.7648	14	63.7888	23	77.2317	15	82.2622	24
	0.05	12.8364	11	21.2958	12	34.5903	13	41.4551	21	49.2868	22	52.4227	14	62.0152	23	74.5602	15	79.3340	24
	0.1	12.6022	11	20.6396	12	32.9442	13	39.3897	21	46.3599	22	48.8927	14	57.4621	23	67.9286	15	72.1582	24
	0.15	12.2463	11	19.6950	12	30.7273	13	36.6382	21	42.5151	22	44.4857	14	51.9457	23	60.2851	15	63.9881	24
	0.2	11.8061	11	18.6005	12	28.3427	13	33.7085	21	38.7801	22	40.0930	14	46.5758	23	53.1956	15	56.4568	24
2/3	0.01	15.5730	11	31.0513	12	44.5274	21	55.3280	13	59.3935	22	83.4671	23	88.2786	14	93.5171	31	107.8902	32
	0.05	15.4495	11	30.5618	12	43.6749	21	53.8568	13	57.8255	22	80.3834	23	84.7336	14	89.9880	31	103.1426	32
	0.1	15.0884	11	29.1996	12	41.3592	21	50.0238	13	53.7714	22	72.8944	23	76.2034	14	81.4322	31	92.0726	32
	0.15	14.5534	11	27.3443	12	38.3196	21	45.3026	13	48.8050	22	64.4583	23	66.7630	14	71.8333	31	80.2016	32
	0.2	13.9113	11	25.3235	12	35.1279	21	40.6583	13	43.9183	22	56.7495	23	58.3074	14	63.0916	31	69.7628	32
1	0.01	23.6327	11	51.6210	21	58.5687	12	86.9792	22	100.0830	31	112.9554	13	133.4419	32	140.4363	23	168.4411	41
	0.05	23.3165	11	50.4086	21	56.8131	12	82.5585	22	95.9681	31	107.0406	13	126.0049	32	131.7770	23	157.5590	41
	0.1	22.4260	11	47.2245	21	52.3247	12	74.4019	22	86.2191	31	93.7048	13	109.8111	32	113.3710	23	134.8340	41
	0.15	21.1863	11	43.2289	21	46.9422	12	65.4110	22	75.5571	31	80.0807	13	93.7048	32	95.6537	23	113.2739	41
	0.2	19.7988	11	39.2032	21	41.7813	12	57.3380	22	66.0322	31	68.6409	13	80.3009	32	81.3218	23	95.9436	41
1.5	0.01	42.4805	11	68.8966	21	115.9983	31	120.6613	12	147.1557	22	183.4637	41	193.0206	32	242.2357	13	258.8632	42
	0.05	41.4044	11	66.5348	21	110.2167	31	113.4983	12	137.1419	22	170.3298	41	177.2548	32	217.4457	13	232.9624	42
	0.1	38.5769	11	60.7549	21	97.2651	31	97.8687	12	116.5230	22	143.9801	41	147.1747	32	173.5875	13	187.6984	42
	0.15	35.0448	11	54.1437	21	82.5178	12	83.9300	31	97.3494	22	113.8782	41	121.0230	32	138.5953	13	150.4991	23
	0.2	31.5267	11	48.0072	21	70.0311	12	72.5296	31	82.2259	22	100.9450	41	101.1634	32	113.6533	13	123.1253	23
2	0.01	69.1986	11	94.3686	21	139.7820	31	205.8509	41	207.3996	12	233.3530	22	277.9620	32	292.1256	51	342.0830	42
	0.05	66.3511	11	89.7039	21	130.9804	31	187.5642	12	188.8981	41	209.2989	22	246.0990	32	261.0176	51	297.6075	42
	0.1	59.4801	11	79.1951	21	112.6778	31	151.1821	12	156.8127	41	167.1253	22	193.5916	32	208.1506	51	229.3521	42
	0.15	51.8607	11	68.3565	21	95.2504	31	121.3015	12	128.9416	41	133.6229	22	153.6213	32	166.4441	51	179.8461	42
	0.2	45.0569	11	59.1227	21	81.1493	31	99.7234	12	107.7263	41	109.7471	22	125.6314	32	136.5442	51	145.9761	42
2.5	0.01	103.6319	11	127.9211	21	171.6985	31	236.0692	41	318.4472	12	320.9089	51	344.0324	22	387.7050	32	425.7568	61
	0.05	97.3935	11	1192.345	21	157.9952	31	213.2347	41	275.2171	12	282.9241	51	295.2020	22	328.9451	32	364.6718	61
	0.1	83.7200	11	101.3485	21	131.7944	31	172.9946	41	208.5001	12	221.8976	51	222.3865	22	245.5162	32	275.9405	61
	0.15	70.2511	11	84.7126	21	108.8771	31	140.1314	41	161.2420	12	171.8160	22	175.7373	51	189.0764	32	212.0670	42
	0.2	59.3130	11	71.6052	21	91.3660	31	116.0146	41	129.7437	12	130.3163	22	143.3802	51	151.9878	32	169.8007	42

Table 3
First nine frequency parameters, $\beta = \omega a^2 \sqrt{\rho h/D}$, for rectangular Mindlin plates: Case 3 (S–C–S–C)

η	δ	1		2		3		4		5		6		7		8		9	
0.4	0.01	12.1316	11	18.3570	12	27.9479	13	40.7131	14	41.3469	21	46.9587	22	56.1158	23	56.6060	15	68.6533	24
	0.05	12.0590	11	18.1764	12	27.5336	13	39.8639	14	40.6226	21	45.9913	22	54.6987	23	55.0253	15	66.5157	24
	0.1	11.8438	11	17.6557	12	26.3750	13	37.5735	14	38.6303	21	43.3940	22	50.9382	15	51.0131	23	61.1531	24
	0.15	11.5174	11	16.9020	12	24.7824	13	34.6025	14	35.9689	21	40.0379	22	45.9577	15	46.4560	23	54.8423	24
	0.2	11.1138	11	16.0217	12	23.0300	13	31.5289	14	33.1265	21	36.5648	22	41.1088	15	41.9312	23	48.8511	24
0.5	0.01	13.6815	11	23.6327	12	38.6587	13	42.5528	21	51.6210	22	58.5687	14	66.2080	23	83.3361	15	85.9792	24
	0.05	13.5802	11	23.3165	12	37.8509	13	41.7720	21	50.4086	22	56.8130	14	64.1675	23	79.9592	15	82.5585	24
	0.1	13.2843	11	22.4260	12	35.6730	13	39.6410	21	47.2245	22	52.3247	14	59.0487	23	71.8320	15	74.4019	24
	0.15	12.8449	11	21.1853	12	32.8480	13	36.8226	21	43.2289	22	46.9422	14	53.0168	23	62.8423	15	65.4110	24
	0.2	12.3152	11	19.7988	12	29.9258	13	33.8397	21	39.2032	22	41.7813	14	47.2796	23	54.8076	15	57.3380	24
2/3	0.01	17.3650	11	35.3123	12	45.3888	21	61.9619	13	62.2293	22	88.6311	23	94.0500	31	97.2091	14	109.8438	32
	0.05	17.1780	11	34.5748	12	44.4590	21	59.8841	13	60.3535	22	84.8364	23	90.4330	31	92.4804	14	104.7439	32
	0.1	16.6455	11	32.5876	12	41.9700	21	54.6728	13	55.6450	22	75.9555	23	81.5726	14	81.7216	31	93.0746	32
	0.15	15.8866	11	30.0089	12	38.7587	21	48.5864	13	50.0790	22	66.3792	23	70.1356	14	72.0080	31	80.7841	32
	0.2	15.0147	11	27.3400	12	35.4346	21	42.8936	13	44.7624	22	57.9303	23	60.3576	14	63.1974	31	70.1036	32
1	0.01	28.9250	11	54.6743	21	69.1986	12	94.3686	22	102.0112	31	128.6906	13	139.7820	32	154.2163	23	169.8080	41
	0.05	28.3324	11	53.1373	21	66.3511	12	89.7039	22	97.5475	31	120.1190	13	130.9804	32	142.6920	23	158.5640	41
	0.1	26.7369	11	49.2606	21	59.4801	12	79.1951	22	87.2072	31	102.0186	13	112.6777	32	119.7031	23	135.3588	41
	0.15	24.6627	11	44.6258	21	51.8607	12	68.3565	22	76.1326	31	84.9044	13	95.2504	32	99.0339	23	113.5394	41
	0.2	22.5099	11	40.1384	21	45.0569	12	59.1227	22	66.3706	31	71.3904	13	81.1493	32	83.1187	23	96.0845	41
1.5	0.01	56.2448	11	78.8093	21	122.8265	31	145.6903	12	169.3605	22	188.3988	41	211.7274	32	274.3277	42	274.5527	51
	0.05	53.9555	11	75.0706	21	115.6043	31	133.7728	12	154.3074	22	173.8255	41	190.6678	32	242.4780	13	243.0197	42
	0.1	48.4087	11	66.6351	21	100.4080	31	110.1837	12	126.1069	22	145.6983	41	153.8021	32	185.2639	13	192.0288	42
	0.15	42.2206	11	57.8782	21	85.6528	31	89.3976	12	102.3338	22	120.7072	41	124.1600	32	143.7580	13	153.0497	42
	0.2	36.6729	11	50.3588	21	73.4961	31	73.7977	12	84.8230	22	101.3700	41	102.6970	32	115.9495	13	124.8211	23
2	0.01	94.9657	11	115.3920	21	155.7139	31	217.8840	41	252.3968	12	275.2751	22	301.4748	51	315.5370	32	374.9280	42
	0.05	88.6635	11	106.9478	21	142.9794	31	197.0426	41	219.5822	12	237.9205	22	266.6247	51	270.0802	32	316.7803	42
	0.1	75.1962	11	90.0396	21	119.1498	31	160.5535	41	166.7806	12	180.2276	22	203.5789	32	210.3605	51	236.4907	42
	0.15	62.3265	11	74.7615	21	96.5933	31	128.3870	12	130.6597	41	139.3327	22	157.7092	32	167.3639	51	182.5724	42
	0.2	52.1283	11	62.9729	21	82.9509	31	102.7371	12	108.5772	41	112.1661	22	127.3254	32	136.9708	51	147.0735	42
2.5	0.01	144.7935	11	163.8759	21	201.0471	31	259.3802	41	339.5056	51	388.7324	12	411.1071	22	440.8641	61	449.9461	32
	0.05	130.8827	11	147.0368	21	178.9088	31	228.2013	41	293.5267	51	318.3346	12	334.8798	22	363.6302	32	372.2524	61
	0.1	104.9093	11	117.2663	21	142.2023	31	179.4027	41	225.4032	12	225.8277	51	237.2521	22	257.6112	32	278.4012	61
	0.15	83.3775	11	93.5703	21	113.9885	31	142.9462	41	167.2978	12	177.0700	22	177.3102	51	193.2199	32	214.7519	61
	0.2	67.8833	11	76.7883	21	94.0516	31	117.3738	41	131.3314	12	139.7953	22	144.0924	51	153.2190	32	170.7370	42

Table 4
First nine frequency parameters, $\beta = \omega a^2 \sqrt{\rho h/D}$, for rectangular Mindlin plates: Case 4 (S–S–S–F)

η	δ	1		2		3		4		5		6		7		8		9	
0.4	0.01	10.1222	11	13.0496	12	18.8228	13	27.5284	14	39.2892	15	39.5761	21	42.6553	22	48.7177	23	54.1731	16
	0.05	10.0713	11	12.9603	12	18.6358	13	27.1525	14	38.5752	15	38.8966	21	41.8689	22	47.6855	23	52.8872	16
	0.1	9.9310	11	12.7247	12	18.1563	13	26.1848	14	36.7312	15	37.0585	21	39.7612	22	44.9842	23	49.6061	16
	0.15	9.7173	11	12.3761	12	17.4706	13	24.8468	14	34.2845	15	36.9691	21	41.4997	22	45.4674	16	48.0301	23
	0.2	9.4470	11	11.9466	12	16.6594	13	23.3345	14	31.6579	15	34.0024	21	37.8894	22	41.2613	16	43.4247	23
0.5	0.01	10.2948	11	14.7549	12	23.5941	13	37.0777	14	39.7326	21	44.4758	22	53.8263	23	55.4110	15	67.7799	24
	0.05	10.2402	11	14.6337	12	23.2979	13	36.4180	14	39.0413	21	43.6095	22	52.5476	23	54.0508	15	65.7675	24
	0.1	10.0929	11	14.3272	12	22.5568	13	34.7428	14	37.1858	21	41.3217	22	49.2886	23	50.6215	15	60.8325	24
	0.15	9.8705	11	13.8833	12	21.5258	13	32.5147	14	34.7029	21	38.3223	22	45.1815	23	46.3254	15	54.9158	24
	0.2	9.5902	11	13.3463	12	20.3423	13	30.1061	14	32.0344	21	35.1634	22	41.0123	23	41.9810	15	49.1758	24
2/3	0.01	10.6655	11	18.2782	12	33.6462	13	40.0898	21	48.3432	22	57.4932	14	64.6033	23	88.9601	24	89.1023	31
	0.05	10.6028	11	18.0794	12	33.0646	13	39.3762	21	47.2942	22	56.0059	14	62.7278	23	85.5180	24	85.8236	31
	0.1	10.4404	11	17.6033	12	31.6345	13	37.4806	21	44.6033	22	52.3231	14	58.1652	23	77.5538	24	77.9373	31
	0.15	10.1988	11	16.9368	12	29.7288	13	34.9551	21	41.1494	22	47.7596	14	52.6627	23	68.6209	24	69.0079	31
	0.2	9.8972	11	16.1546	12	27.6476	13	32.2485	21	37.5758	22	43.1813	14	47.2839	23	60.4233	24	61.2471	15
1	0.01	11.6746	11	27.7042	12	41.1469	21	58.9430	22	61.7308	13	90.1079	31	94.1917	23	108.6295	32	115.3773	14
	0.05	11.5877	11	27.2439	12	40.3718	21	57.3087	22	59.9760	13	86.7166	31	90.2271	23	103.7154	32	109.9606	14
	0.1	11.3810	11	26.1910	12	38.3610	21	53.3852	22	55.7620	13	78.6490	31	81.3690	23	92.5861	32	97.7407	14
	0.15	11.0843	11	24.7933	12	35.7110	21	48.6013	22	50.6444	13	69.5645	31	71.6390	23	80.6821	32	84.7846	14
	0.2	10.7218	11	23.2429	12	32.8922	21	43.8679	22	46.6862	13	61.2416	31	62.8294	23	70.2031	32	73.4143	14
1.5	0.01	13.6902	11	43.5028	21	47.7345	12	81.2001	22	92.4741	31	124.1821	13	132.3816	32	158.1694	23	160.8479	41
	0.05	13.5441	11	42.5886	21	46.5188	12	78.0153	22	88.8342	31	117.8897	13	124.9498	32	147.8047	23	150.6618	41
	0.1	13.2343	11	40.3170	21	43.7524	12	71.0199	22	80.3498	31	104.0594	13	109.3530	32	127.0726	23	129.5337	41
	0.15	12.8130	11	37.3871	21	40.3149	12	63.1636	22	70.9025	31	89.6929	13	93.6847	32	107.1792	23	109.2717	41
	0.2	12.3167	11	34.3172	21	36.7879	12	55.8742	22	62.3103	31	77.2283	13	80.4796	32	90.8391	23	92.8373	41
2	0.01	16.0971	11	46.6393	21	75.0554	12	95.7777	31	110.5044	22	163.8087	32	164.1500	41	211.1602	13	234.7995	42
	0.05	15.8630	11	45.5242	21	72.3859	12	91.7889	31	104.7642	22	152.4308	32	153.4438	41	194.5058	13	213.5408	42
	0.1	15.4054	11	42.8870	21	66.3720	12	82.7190	31	92.9718	22	130.3462	32	131.5689	41	162.3547	13	175.4315	42
	0.15	14.8112	11	39.5731	21	59.4250	12	72.7642	31	80.7070	22	109.5805	32	110.7739	41	133.4920	13	143.0749	42
	0.2	14.1341	11	36.1646	21	52.8012	12	63.7960	31	69.9757	22	92.8079	32	93.9941	41	110.5435	13	118.7291	42
2.5	0.01	18.7406	11	50.4009	21	99.9102	31	109.8392	12	146.7800	22	168.3842	41	202.3165	32	256.0054	51	275.2534	42
	0.05	18.3895	11	49.0194	21	95.4674	31	104.6127	12	137.1854	22	157.0074	41	185.3216	32	231.7630	51	246.4233	42
	0.1	17.7395	11	45.9146	21	85.6500	31	93.2356	12	118.5437	22	134.1717	41	154.6262	32	188.6209	51	198.1884	42
	0.15	16.9249	11	42.1227	21	75.0566	31	81.0910	12	100.4748	22	112.6931	41	127.5138	32	152.8319	51	159.2575	42
	0.2	16.0212	11	38.2999	21	65.6190	31	70.2224	12	85.3984	22	95.4702	41	106.3776	32	126.4017	51	130.6939	42

Table 5
First nine frequency parameters, $\beta = \omega a^2 \sqrt{\rho h/D}$, for rectangular Mindlin plates: Case 5 (S–F–S–F)

η	δ	1		2		3		4		5		6		7		8		9	
0.4	0.01	9.7569	11	11.0297	12	15.0461	13	21.6744	14	31.1252	15	39.2043	21	40.4594	22	43.5927	16	44.8844	23
	0.05	9.7107	11	10.9587	12	14.9033	13	21.3894	14	30.5968	15	39.5389	21	39.7240	22	42.6585	16	43.9728	23
	0.1	9.5814	11	10.7809	12	14.5672	13	20.7245	14	29.3338	15	36.7363	21	37.7879	22	40.3787	16	41.6202	23
	0.15	9.3833	11	10.5199	12	14.0936	13	19.8152	14	27.6516	15	34.3132	21	35.2188	22	37.4463	16	38.5619	23
	0.2	9.1313	11	10.1968	12	13.5287	13	18.7728	14	25.8016	15	31.7000	21	32.4730	22	34.3696	16	35.3558	23
0.5	0.01	9.7328	11	11.6746	12	17.6584	13	27.7042	14	39.1526	21	41.1469	22	42.2999	15	47.8924	23	58.9430	24
	0.05	9.6858	11	11.5877	12	17.4479	13	27.2440	14	38.4845	21	40.3718	22	41.3784	15	46.8244	23	57.3087	24
	0.1	9.5560	11	11.3811	12	16.9766	13	26.1910	14	36.6824	21	38.3610	22	39.1884	15	44.1468	23	53.3852	24
	0.15	9.3578	11	11.0842	12	16.3322	13	24.7933	14	34.2626	21	35.7110	22	36.3834	15	40.7299	23	48.6013	24
	0.2	9.1061	11	10.7218	12	15.5826	13	23.2429	14	31.6538	21	32.8922	22	33.4360	15	37.2004	23	43.8579	24
2/3	0.01	9.6945	11	12.9648	12	22.9038	13	39.0679	21	40.2602	14	42.6228	22	54.1237	23	66.0689	15	72.9810	24
	0.05	9.6463	11	12.8416	12	22.5355	13	38.3955	21	39.3568	14	41.7615	22	52.6938	23	64.0286	15	70.4130	24
	0.1	9.5157	11	12.5711	12	21.7490	13	36.5941	21	37.3019	14	39.5886	22	49.2912	23	59.2503	15	64.6182	24
	0.15	9.3175	11	12.1967	12	20.7148	13	34.1797	21	34.6910	14	36.7640	22	45.0990	23	53.5523	15	57.9316	24
	0.2	9.0666	11	11.7505	12	19.5561	13	31.5782	21	31.9427	14	33.7882	22	40.8870	23	47.9953	15	51.5921	24
1	0.01	9.6270	11	16.0971	12	36.6112	13	38.9043	21	46.6393	22	70.4846	23	75.0554	14	87.8151	31	95.7777	32
	0.05	9.5771	11	15.8630	12	35.7400	13	38.2240	21	45.5242	22	67.9066	23	72.3859	14	84.6068	31	91.7889	32
	0.1	9.4458	11	15.4054	12	33.9160	13	36.4246	21	42.8870	22	62.3304	23	66.3720	14	76.9042	31	82.7190	32
	0.15	9.2484	11	14.8112	12	31.6442	13	34.0208	21	39.5731	22	55.9480	23	59.4250	14	68.1629	31	72.7642	32
	0.2	8.9997	11	14.1341	12	29.2558	13	31.4338	21	36.1646	22	49.8953	23	52.8012	14	60.1064	31	63.7960	32
1.5	0.01	9.5535	11	21.5305	12	38.6764	21	54.6518	22	65.5402	13	87.4436	31	103.3677	23	104.7633	32	152.1523	14
	0.05	9.5030	11	21.0333	12	37.9868	21	52.9372	22	63.2537	13	84.2198	31	97.8722	23	99.7582	32	142.7898	14
	0.1	9.3729	11	20.1451	12	36.1927	21	49.2667	22	58.4124	13	76.5468	31	87.0907	23	89.0395	32	123.4724	14
	0.15	9.1787	11	19.0615	12	33.8064	21	44.9105	22	52.8207	13	67.8548	31	75.9074	23	77.6896	32	104.3945	14
	0.2	8.9345	11	17.8846	12	31.2425	21	40.6053	22	47.4411	13	59.8469	31	66.0798	23	67.6996	32	88.1197	14
2	0.01	9.5078	11	27.3597	12	38.4774	21	64.2036	22	87.0926	31	105.0353	13	116.2287	32	145.8142	23	155.2404	41
	0.05	9.4583	11	26.4801	12	37.7831	21	61.6215	22	83.8573	31	100.0269	13	109.7706	32	135.6642	23	145.6983	41
	0.1	9.3306	11	24.9711	12	35.9987	21	56.5363	22	76.2163	31	89.5926	13	96.8198	32	117.0233	23	125.7350	41
	0.15	9.1402	11	23.1961	12	33.6339	21	50.8097	22	67.5758	31	78.5665	13	83.6442	32	99.2701	23	106.3946	41
	0.2	8.9007	11	21.3271	12	31.0963	21	45.3418	22	59.6198	31	68.8138	13	72.3227	32	84.6280	23	90.5962	41
2.5	0.01	9.4797	11	33.3642	12	38.3130	21	74.6758	22	86.7681	31	129.4716	32	154.7650	41	155.3634	13	198.1144	23
	0.05	9.4315	11	31.9757	12	37.6187	21	70.9578	22	83.5270	31	121.1250	32	145.2186	41	145.5793	13	181.0380	23
	0.1	9.3065	11	29.6389	12	35.8486	21	64.0850	22	75.9234	31	105.4121	32	125.3334	41	126.1938	13	151.4692	23
	0.15	9.1193	11	26.9579	12	33.5079	21	56.6669	22	67.3397	31	90.0267	32	106.0845	41	107.5585	13	125.4338	23
	0.2	8.8835	11	24.2054	12	30.9976	21	49.7609	22	59.4404	31	77.0654	32	90.3658	41	92.2433	13	105.0932	23

Table 6
First nine frequency parameters, $\beta = \omega a^2 \sqrt{\rho h/D}$, for rectangular Mindlin plates: Case 6 (S–C–S–F)

η	δ	1		2		3		4		5		6		7		8		9	
0.4	0.01	10.1848	11	13.5947	12	20.0776	13	29.5868	14	39.6021	21	42.1851	15	42.9565	22	49.5127	23	57.9108	16
	0.05	10.1319	11	13.4887	12	19.8437	13	29.1124	14	38.9107	21	41.2893	15	42.1449	22	48.4091	23	56.3209	16
	0.1	9.9871	11	13.2121	12	19.2456	13	27.8944	14	37.0765	21	38.9971	15	39.9820	22	45.5522	23	52.3237	16
	0.15	9.7676	11	12.8087	12	18.4063	13	26.2480	14	34.6080	21	36.0362	15	37.1334	22	41.9122	23	47.4327	16
	0.2	9.4910	11	12.3200	12	17.4363	13	24.4379	14	31.9525	21	32.9523	15	34.1210	22	38.1799	23	42.6163	16
0.5	0.01	10.4206	11	15.7393	12	25.7574	13	39.7874	21	40.5324	14	45.0551	22	55.2982	23	60.1784	15	70.3559	24
	0.05	10.3618	11	15.5842	12	25.3653	13	39.0904	21	39.6621	14	44.1381	22	53.8756	23	58.4177	15	68.0502	24
	0.1	10.2054	11	15.1956	12	24.3830	13	37.2242	21	37.4665	14	41.7409	22	50.3101	23	54.0543	15	62.5113	24
	0.15	9.9712	11	14.6443	12	23.0502	13	34.6374	14	34.7311	21	38.6310	22	45.9063	23	48.7890	15	56.0469	24
	0.2	9.6782	11	13.9934	12	21.5678	13	31.6896	14	32.0545	21	35.3839	22	41.5112	23	43.6674	15	49.9152	24
2/3	0.01	10.9682	11	20.3073	12	37.8901	13	40.2293	21	49.6579	22	64.0609	14	67.7516	23	89.1850	31	94.2461	24
	0.05	10.8951	11	20.0257	12	37.0603	13	39.5018	21	48.4841	22	61.9924	14	65.5195	23	85.8902	31	90.0643	24
	0.1	10.7099	11	19.3498	12	35.0192	13	37.5793	21	46.5302	22	56.9754	14	60.2293	23	77.9793	31	80.6773	24
	0.15	10.4390	11	18.4298	12	32.4007	13	35.0275	21	41.8180	22	51.0561	14	54.0632	23	69.0335	31	70.5727	24
	0.2	10.1060	11	17.3888	12	29.6707	13	32.3003	21	38.0442	22	45.4110	14	48.2070	23	61.6093	24	63.2764	15
1	0.01	12.6728	11	32.9925	12	41.6472	21	62.8595	22	72.2171	13	90.4194	31	102.7904	23	111.5689	32	130.9964	14
	0.05	12.5482	11	32.2370	12	40.8218	21	60.7824	22	69.4393	13	86.9701	31	97.5322	23	106.1105	32	123.0672	14
	0.1	12.2606	11	30.4743	12	38.7128	21	55.9736	22	62.9527	13	78.8120	31	86.2713	23	94.0906	32	106.1656	14
	0.15	11.8620	11	28.2362	12	35.9677	21	50.3782	22	55.6218	13	69.6629	31	74.6338	23	81.5621	32	89.6189	14
	0.2	11.3931	11	25.8975	12	33.0747	21	45.0445	22	48.8911	13	61.3014	31	64.6148	23	70.7202	32	76.0573	14
1.5	0.01	16.7875	11	45.2148	21	60.8312	12	91.9180	22	93.5911	31	141.1267	32	149.0012	13	161.6466	41	180.1544	23
	0.05	16.5179	11	44.1176	21	58.4647	12	87.1780	22	89.7406	31	131.7987	32	138.3211	13	151.2366	41	164.9217	23
	0.1	15.9404	11	41.4965	21	53.0869	12	77.3057	22	80.9273	31	113.3509	32	116.7400	13	129.8348	41	136.6792	23
	0.15	15.1913	11	38.2377	21	46.9606	12	67.0994	22	71.2484	31	95.8630	32	96.8123	13	109.4262	41	112.0940	23
	0.2	14.3646	11	34.9199	21	41.2635	12	58.2641	22	62.5203	31	81.1835	13	81.6739	32	92.9209	41	93.3381	23
2	0.01	22.7512	11	50.6057	21	98.4649	31	99.3823	12	131.4853	22	166.1173	41	181.7921	32	250.1932	42	253.2971	51
	0.05	22.2469	11	49.0424	21	93.5256	12	93.9506	31	121.8970	22	154.8514	41	165.8679	32	223.8942	42	227.2697	13
	0.1	21.1870	11	45.5725	21	81.0357	12	84.0786	31	103.5900	22	132.2990	41	137.5355	32	178.6892	13	180.1780	42
	0.15	19.8705	11	41.5047	21	68.4310	12	73.5755	31	86.6229	22	111.1472	41	113.1589	32	141.1201	13	145.1981	42
	0.2	18.4903	11	37.5487	21	57.8767	12	64.2947	31	73.0862	22	94.1986	41	94.5611	32	114.5430	13	119.7053	42
2.5	0.01	30.5270	11	57.8545	21	105.1242	31	148.7010	12	172.2784	41	181.4601	22	232.9375	32	259.0458	51	302.2416	42
	0.05	29.6813	11	55.5986	21	99.6242	31	136.3896	12	159.7670	41	163.9473	22	206.9864	32	233.6515	51	263.6216	42
	0.1	27.8981	11	50.9077	21	88.2403	31	112.4394	12	133.2557	22	135.5890	41	165.0990	32	189.4319	51	205.4196	42
	0.15	25.7584	11	45.7332	21	76.6139	31	91.0054	12	107.5361	22	113.4230	41	132.1264	32	153.2002	51	162.1838	42
	0.2	23.6105	11	40.9415	21	66.6065	31	74.5669	12	88.3290	22	95.8842	41	108.2063	32	126.5933	51	131.8118	42

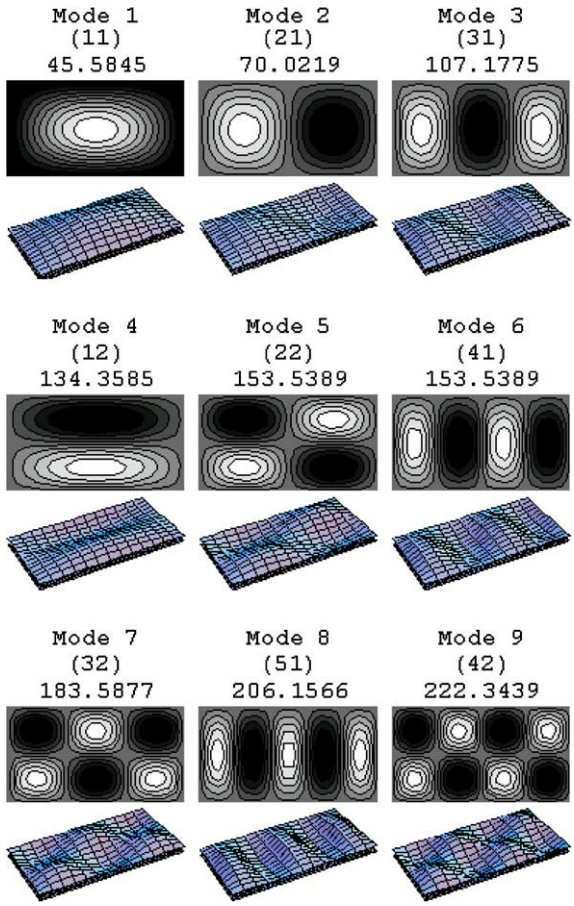

Fig. 3. First nine mode shapes of S–S–S–S rectangular plate ($\eta = 2$, $\delta = 0.1$, $v = 0.3$).

sinusoidal. A consequence of this result as it can be observed in Figs. 3–8 is that the nodal lines lying in the x_2-direction (three for a 41 mode) are evenly spaced. On the other hand those lying in the x_1-direction (two for a 13 mode), except for the S–S–S–S case, and except for an axis of symmetry are not evenly spaced.

To avoid any confusion it is pertain to mention that the phrase 'nodal line' should be interpreted as line across which there is no transverse displacement whether or not accompanied with zero in-plane displacement components.

For purpose of subsequent discussion in this section it is also useful to clarify some terminology with respect to symmetry of modes. As already used in Section 3, x_2-symmetric modes are those modes having an axis of symmetry with respect to the x_2 -coordinate (e.g., 11, 21, 31, 13, 51 modes are x_2-symmetric). Similarly, for example, the 12, 22, 32, 42 and 14 modes are x_2-antisymmetric modes. Accordingly as it can be observed by examining the counter pots In Figs. 3–8 the above examples of x_2-symmetric and x_2-antisymmetric modes are only true where double geometric symmetry exist (e.g., S–S–S–S, S–C–S–C, S–F–S–F). In another word as it can be clearly seen in Figs. 6 and 8 the 11, 21, 31 and 13 modes are not correct examples of the x_2-symmetric modes where double geometric symmetry does not exist.

The close examination of the counter plots also suggests that the modes can be classified into four distinct symmetry classes: namely, double-symmetry modes (SS), symmetry–antisymmetry modes (SA),

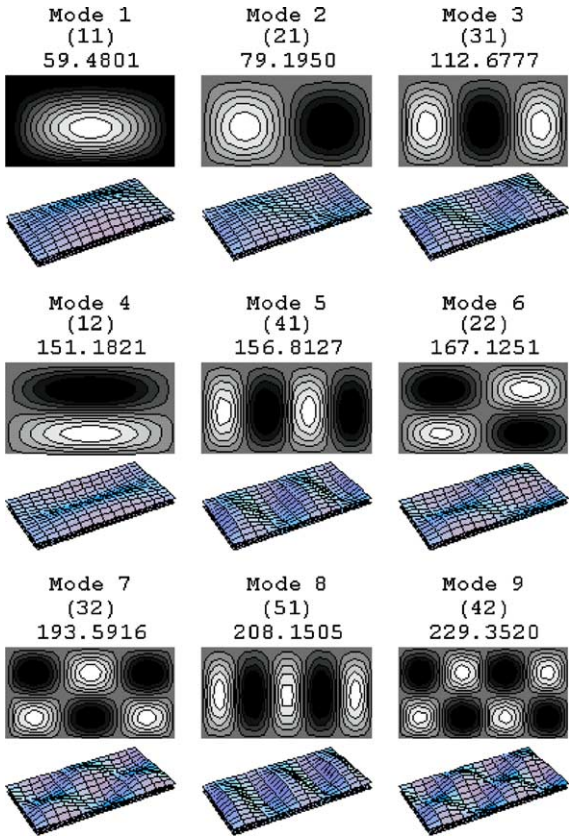

Fig. 4. First nine mode shapes of S–C–S–S rectangular plate ($\eta = 2$, $\delta = 0.1$, $v = 0.3$).

antisymmetry–symmetry modes (AS) and double antisymmetry modes (AA), about the midplanes parallel to the x_1-x_3 and x_2-x_3 planes. According to these symmetry classes (11, 31, 51), (21, 41), (12, 32) and (22, 42) modes in Fig. 3 may be given as an examples of SS, SA, AS and AA modes, respectively.

In order to study the effects of boundary conditions, plate aspect ratio and relative thickness ratio on the vibrational behavior of the rectangular plates, considerations may now be focused on Tables 1–6. From the results presented in these Tables, it is observed that the frequency parameters increase with increasing plate aspect ratio η if the relative thickness ratio δ and boundary conditions are kept constant.

The influence of thickness ratio on the frequency parameters for plates with specific boundary conditions can also be examined by keeping the aspect ratio constant while varying the thickness ratio. As a result it can be easily observed that, as the thickness ratio δ increases from 0.01 to 0.2, the frequency parameter decreases. The decrease in the frequency parameter is due to effects of shear deformation and rotatory inertia. These effects are more pronounced in the higher modes than in the lower modes.

To study the effect of the boundary conditions on the vibration characteristic of thick plates, the frequency parameters listed in a specific row of Tables 1–6 may be selected from each table and arranged in terms of boundary conditions as Table 7. From the results presented in this table, it is observed that the lowest frequency parameters correspond to plates subject to less edge restraints. As the number of supported edges increases, the frequency parameters also increase. Among all six boundary conditions listed in Table 7, it can be seen that the lowest and highest values of frequency parameters correspond to S–F–S–F

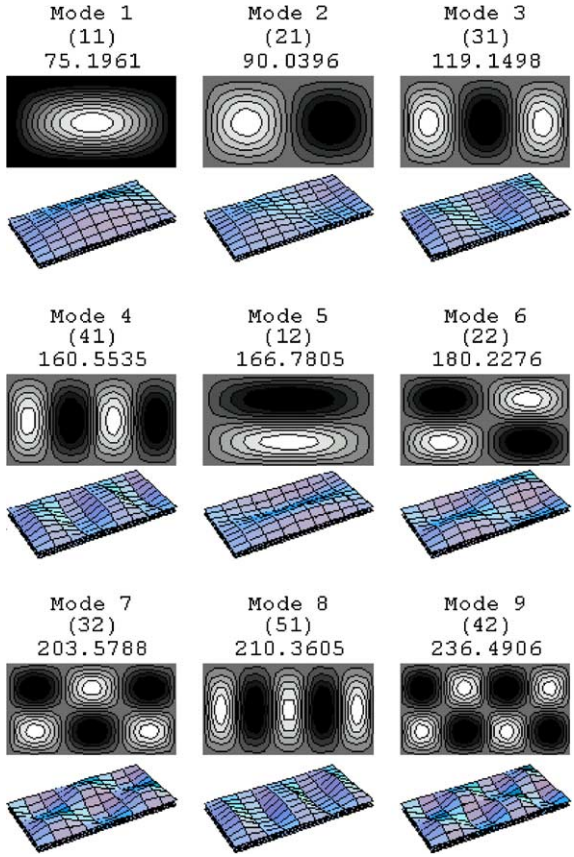

Fig. 5. First nine mode shapes of S–C–S–C rectangular plate ($\eta = 2$, $\delta = 0.1$, $\nu = 0.3$).

and S–C–S–C cases, respectively. Thus higher constraints at the edges increase the flexural rigidity of the plate, resulting in a higher frequency response.

4.1. Complementary results

Further results may also be gleaned from present work regarding nodal lines, existence of eigenvalues such that $\alpha_1 < m\pi$ and some specifications of individual cases as given below.

4.1.1. S–S–S–S

In order for Eq. (18) to be satisfied it is necessary that $\lambda_1 = n\pi$, with integer values of n. Thus for this case (and only this case), the nondimensional frequency parameter can be determined explicitly; i.e.

$$\beta^2 = \frac{72 v_1 K^2}{\delta^4}\left\{1 + \frac{\delta^2\tilde{\beta}}{12}\left(1 + \frac{1}{v_1 K^2}\right) - \sqrt{\left[1 + \frac{\delta^2\tilde{\beta}}{12}\left(1 + \frac{1}{v_1 K^2}\right)\right]^2 - \frac{\delta^4\tilde{\beta}^2}{36 v_1 K^2}}\right\}, \tag{47a}$$

where

$$\tilde{\beta} = \pi^2(m^2 + n^2\eta^2), \tag{47b}$$

is the frequency parameter of the corresponding simply supported thin plate.

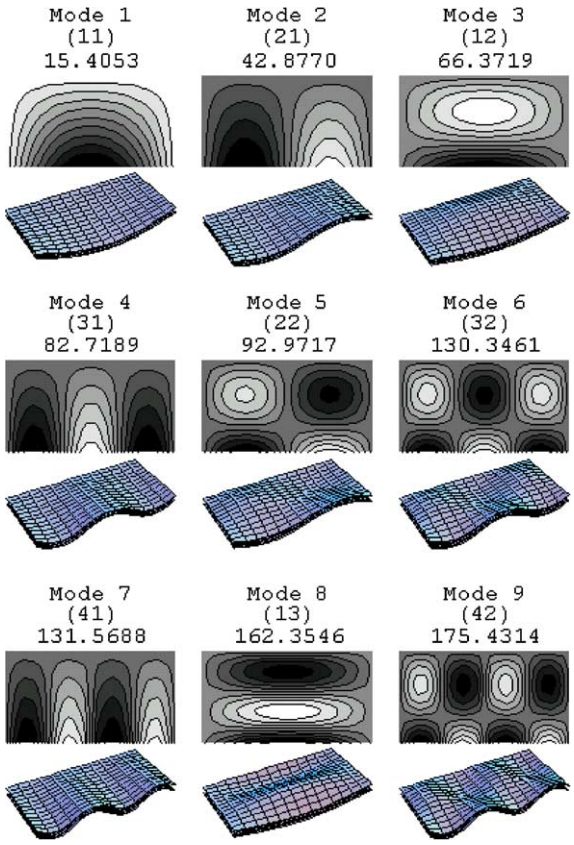

Fig. 6. First nine mode shapes of S–S–S–F rectangular plate ($\eta = 2$, $\delta = 0.1$, $v = 0.3$).

Inspection of frequency parameters listed in Table 1 reveals that, for example, the 12 mode for $\eta = 0.5$ and $\delta = 0.1$ corresponds to the 11 mode of a plate having $\eta = 1$ and the same values of δ and frequency parameter. Similarly the 14, 22 and 24 modes of the former plate correspond to the 12, 21 and 22 modes of the latter plate having the same values of δ and frequency parameters, respectively. This is because the conditions along axis of symmetry and evenly spaced nodal lines are the same as those of simply supported edge. In other word, for example, there are three evenly spaced nodal lines at position $X_2 = 0.25, 0.5, 0.75$ for the 24 mode of S–S–S–S plate. Considering only quarter of the plate in this mode, one then has an S–S–S–S plate with aspect ratio 4η vibrating in the 21 mode, with the same frequency as the plate with aspect ratio η.

Consider now two S–S–S–S plates with same frequency parameters and different aspect ratios namely η and η^*. Upon using Eq. (25b)one may easily writes

$$\eta^2 n^2 + m^2 = (\eta^*)^2 (n^*)^2 + (m^*)^2. \tag{48}$$

For the same number of half waves in the x_1-direction ($m^* = m$), Eq. (48) may be written as

$$\frac{n}{\eta^*} = \frac{n^*}{\eta}. \tag{49}$$

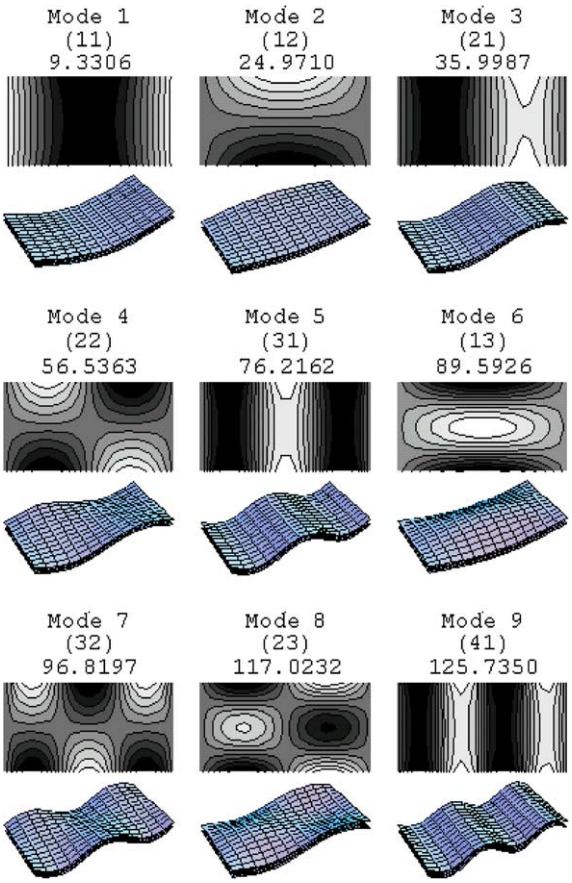

Fig. 7. First nine mode shapes of S–F–S–F rectangular plate ($\eta = 2$, $\delta = 0.1$, $v = 0.3$).

Eq. (49) may now be used to describe the modes of plates with the same frequency parameters as their aspect ratios and their number of half waves in the x_2-direction vary. As an example, the 24 mode for $\eta = 0.5$ and $\delta = 0.15$ (with $\beta = 62.6035$) can be interpreted as the 21 mode for $\eta^* = 2$, or as the 22 mode for $\eta^* = 1$ with the same δ and β, by rewriting Eq. (49) in the form

$$\frac{n}{\eta^*} = \frac{n^*}{\eta} = \frac{4}{2} = \frac{1}{0.5} = \frac{2}{1} = \cdots. \tag{50}$$

Obviously many divided numbers have the same ratio as expression (50) and there are many values of n and η which satisfy Eq. (49). Hence considerable additional results regarding other aspect ratios not covered in Table 1, can be obtained from the same table. For example the 31 and 32 modes for $\eta = 1.5$ give the frequency parameters for the 36 and 31 modes of plates having $\eta^* = 0.25$ and $\eta^* = 3$, respectively.

To describe the modes of identical frequencies for $\eta^* = \eta$, Eq. (48) can be written as

$$\frac{m}{n^*} = \frac{m^*}{n} = \eta. \tag{51}$$

Upon making use of this equation for $\eta = 1$, one may writes

$$\frac{m}{n^*} = \frac{m^*}{n} = 1 = \frac{1}{1} = \frac{2}{2} = \frac{3}{3} = \cdots. \tag{52}$$

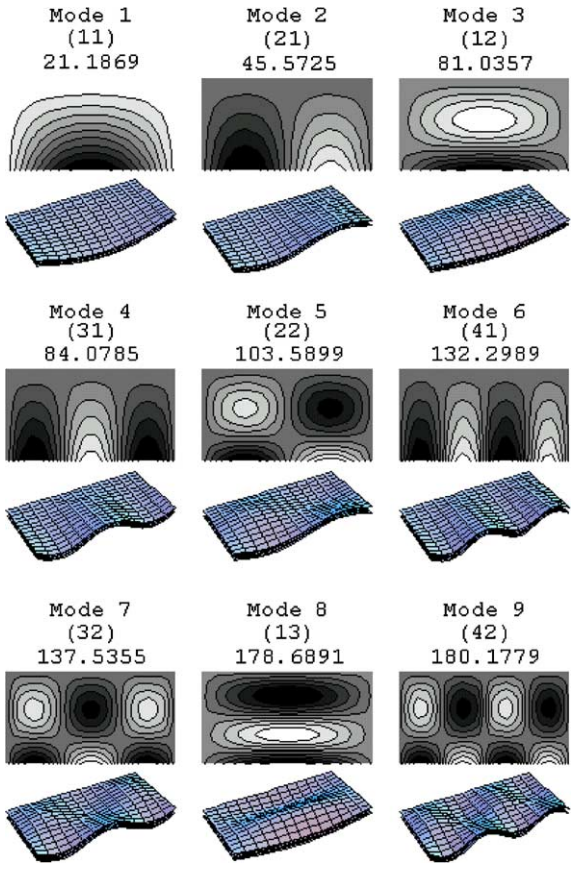

Fig. 8. First nine mode shapes of S–C–S–F rectangular plate ($\eta = 2$, $\delta = 0.1$, $\nu = 0.3$).

Table 7
Frequency parameters for thick plates with different boundary conditions ($\eta = 0.5$, $\delta = 0.2$)

Boundary conditions	Mode sequences								
	1	2	3	4	5	6	7	8	9
S–F–S–F	9.1061	10.7218	15.5826	23.2429	31.6538	32.8922	33.4360	37.2004	43.8579
S–S–S–F	9.5902	13.3463	20.3423	30.1061	32.0344	35.1634	41.0123	41.9810	49.1758
S–C–S–F	9.6782	13.9934	21.5678	31.6896	32.0545	35.3839	41.5112	43.6674	49.9152
S–S–S–S	11.3961	17.5055	26.7944	33.5896	38.3847	38.3847	45.8969	51.5392	55.5860
S–C–S–S	11.8061	18.6005	28.3427	33.7085	38.7801	40.0930	46.5758	53.1956	56.4568
S–C–S–C	12.3152	19.7988	29.9258	33.8397	39.2032	41.7813	47.2796	54.8076	57.3380

Thus within the nine lowest values of β for $\eta = 1$, the coupled modes are (12, 21), (13, 31) and (23, 32).

Eq. (48) may also be used to describe the modes of identical frequencies with same number of half waves in the x_2-direction ($n^* = n$). In this case Eq. (48) can be expressed as

$$\frac{m}{\eta^*} = \frac{m^*}{\eta} = n. \tag{53}$$

As an example, for $n = 1$ Eq. (53) may be given as

$$\frac{m}{\eta^*} = \frac{m^*}{\eta} = 1 = \frac{1}{1} = \frac{2}{2} = \cdots. \tag{54}$$

Thus one may conclude that, the 11 mode for $\eta = 2$ and the 21 mode for $\eta^* = 1$ have an identical frequencies. In order to interpret these modes, imagine a vibrating plate having $\eta = 1$ and taking into consideration that, the 21 and 12 modes are the coupled modes. The 12 mode has a nodal line along $X_2 = 1/2$. Keeping the length fixed and halving the width, the aspect ratio would be doubled. Therefore, the 11 mode for the plate having $\eta = 2$ can be interpreted as whether the 12 or 21 modes of plate having $\eta^* = 1$, all vibrating with an identical frequency.

Consider now two S–S–S–S plates with different frequency parameters. Using Eq. (25b) one obtains

$$\alpha_1^2 = n^2\pi^2\eta^2 + m^2\pi^2, \quad (\alpha_1^*)^2 = (n^*)^2\pi^2(\eta^*)^2 + (m^*)^2\pi^2. \tag{55a,b}$$

Combining Eqs. (55a) and (55b) for the same number of half waves in the x_2-direction ($n^* = n$), gives

$$\frac{\alpha_1^*}{\alpha_1} = \frac{m^*}{m} = \frac{\eta^*}{\eta}. \tag{56}$$

Knowing the ratio η^*/η, the frequency parameters of two plates can be related as

$$(\beta^*)^2\left(a_1 + \sqrt{a_2^2 + \frac{4}{(\beta^*)^2}}\right) = \left(\frac{\eta^*}{\eta}\right)^2\beta^2\left(a_1 + \sqrt{a_2^2 + \frac{4}{\beta^2}}\right), \tag{57}$$

where

$$a_1 = \frac{\delta^2}{12}\left(\frac{1}{K^2\nu_1} + 1\right), \quad a_2 = \frac{\delta^2}{12}\left(\frac{1}{K^2\nu_1} - 1\right). \tag{58a,b}$$

Once again because the conditions along evenly spaced nodal lines are the same as those of simply supported edge, additional results for other η may be obtained from Table 1. For example, consider the S–S–S–S plate having $\eta = 2$ and $\delta = 0.15$. The 21 mode has a nodal line along $X_1 = 1/2$ and has $\beta = 62.6035$. Considering only one-half of the plate in this mode, one then has an S–S–S–S plate with $\eta^* = 1$ vibrating in the 11 mode. Substituting for a_1, a_2, β and η^*/η into Eq. (57) yields, $\beta^* = 18.3661$ (already given in Table 1).

Alternatively by selecting $\eta^* = 1$, Eq. (56) for a plate having $\eta = 2$ and vibrating in 21 mode may be written as

$$\frac{\alpha_1^*}{\alpha_1} = \frac{m^*}{m} = \frac{\eta^*}{\eta} = \frac{1}{2} = \frac{1}{2}\cdots, \tag{59}$$

which in turn indicates that 21 mode for $\eta = 2$ corresponds to the 11 mode for $\eta^* = 1$. Similarly by selecting $\eta^* = 5/6$ and $\delta = 0.15$ the 31 mode for $\eta = 2.5$ yields the fundamental (11 mode) frequency for the selected plate, vibrating with $\beta^* = 15.7191$ (not covered in Table 1).

Finally, it is pertain to mention that as shown in Appendix B, Eq. (27) for $\alpha_1 < m\pi$ has no roots.

4.1.2. S–C–S–S and S–C–S–C

The position of the nodal lines along the x_2 axis for the S–C–S–S plate may be obtained from Eq. (38), by simply equating the X_2 dependent function to zero. As an example the position of the nodal lines within the first nine modes whose frequency parameters for $\eta = 2$ and $\delta = 0.1$ are listed in Table 2 may be found to be at $X_2 = 0.4599$, 0.4665, 0.4737, 0.4799 for 12, 22, 32 and 42 modes, respectively.

A consequence of these results is that the nodal lines lying in the x_1-direction are not evenly spaced, due to nonsinusoidal form of X_2 dependent function. Thus the conditions along these nodal lines are not the same as those of a simply supported edge.

Unlike the nodal lines lying in the x_1-direction, those lying in the x_2-direction are evenly spaced. This is because the x_1 dependent function is sine function exactly.

Additional results for vibration frequencies of S–C–S–S plates can be found quite simply from the x_2-antisymmetric results for S–C–S–C plates given in Table 3. Inspecting data given in Tables 2 and 3, one observes that 14 mode for an S–C–S–C plate having $\eta = 0.5$ and $\delta = 0.15$ corresponds to the 12 mode for an S–C–S–S plate having $\eta = 1$, $\delta = 0.15$ and the same value of frequency parameter, $\beta = 46.9422$.

In order to interpret this observation one may imagine an S–C–S–C plate having $\eta = 0.5$ and $\delta = 0.15$ vibrating in the 14 mode. For the 14 mode of a plate with the same specification as above the position of the nodal lines lying in the x_1-direction may be found from Eq. (39) to be at $X_2 = 0.2697$, 0.5, 0.7302. Unlike the S–S–S–S plate, these nodal lines are not evenly spaced. But the nodal line at position $X_2 = 0.5$ is one of geometrical symmetry. As a result the conditions along the nodal line positioned at $X_2 = 0.5$ are the same as those simply supported edge only.

Keeping the length of plate fixed and halving the width, the aspect ratio would be doubled. Thus one has an S–C–S–S plate with $\eta = 1$ vibrating in the 12 mode and having the same frequency parameter as the 14 mode of S–C–S–C plate with $\eta = 0.5$.

Accordingly additional results for S–C–S–S plates having $\eta = 0.8$, 4/3, 3, 4 and 5 may be obtained from the x_2-antisymmetric data given in Table 3. Similarly additional results for x_2-antisymmetric modes of S–C–S–C plates having $\eta = 0.2$, 0.25, 1/3, 0.75 and 1.25 can be gleaned from the data given in Table 2.

Finally as far as the existence of the eigenvalues with $\alpha_1 < m\pi$ is concerned, as shown in Appendix B, Eqs. ((28), (35c) and (35d) for $\alpha_1 < m\pi$ have no roots.

4.1.3. S–S–S–F, S–F–S–F and S–C–S–F

In Appendix B, it is found that as far as the x_2-symmetric modes of S–F–S–F plate are concerned, there always exists one x_2-symmetric mode for each value of m such that $\alpha_1 < m\pi$. It is also shown that the characteristic equations given for S–S–S–F, S–C–S–F and x_2-antisymmetric modes of S–F–S–F plates in case $\alpha_1 < m\pi$ have roots, if a certain condition established individually for each case to be satisfied.

The lowest integer values of m satisfying the corresponding condition for each case are listed in Table 8 for different values of η and δ. From the results presented in this table one observes that as η increases, m also increases. The lowest value of m corresponds to $\eta = 0.4$ and its highest value corresponds to $\eta = 2.5$. Inspection of data given in Table 8, also reveal that, except for the x_2-symmetric

Table 8
The lowest integer values of m satisfying the condition $f(\beta^*) < g(\beta^*)$

	S–S–S–F							S–F–S–F							S–C–S–F						
η	0.4	0.5	2/3	1	1.5	2	2.5	0.4	0.5	2/3	1	1.5	2	2.5	0.4	0.5	2/3	1	1.5	2	2.5
δ	$m \geqslant$							$m \geqslant$							$m \geqslant$						
0.01	3	4	5	7	10	13	16	6	7	9	13	18	23	28	3	4	5	7	10	13	16
0.05	3	4	4	6	8	10	12	5	6	7	10	15	19	23	3	4	5	6	8	11	13
0.1	3	3	4	5	8	10	12	5	5	7	10	14	19	24	3	3	4	6	8	10	12
0.15	3	3	4	5	7	10	12	4	5	7	10	15	19	22	3	3	4	5	7	10	12
0.2	3	3	4	5	7	10	12	4	5	7	10	14	18	20	3	3	4	5	7	10	12

modes of S–F–S–F plate, no frequencies of $\alpha_1 < m\pi$ type appear among the first nine, for the values of η used in Tables 4–6.

It is also interesting to note that similar to S-S-S-C and S–C–S–C plates, additional results for S–S–S–F plate may be obtained from the x_2-antisymmetric data for S–F–S–F plate and vice versa.

Table 9
Comparison study of frequency parameters $\beta = \omega a^2\sqrt{\rho h/D}$ for square Mindlin plates with S–S–S–S boundaries

δ	Method	Mode sequences								
		1	2	3	4	5	6	7	8	9
0.001	Leissa (1973)	19.7392	49.3480	49.3480	78.9568	98.6960	98.6960	128.3049	128.3049	167.7833
	Liew et al. (1993a)	19.7392	49.3480	49.3480	78.9568	98.6951	98.6951	128.3030	128.3030	167.7780
	Liew et al. (1995a)	19.7392	49.3480	49.3480	78.9568	98.6960	98.6960	128.3050	128.3050	–
	Present[a]	19.7391	49.3475	49.3475	78.9557	98.6943	98.6934	128.3019	128.3019	167.7782
0.1	Liew et al. (1993a)	19.0651	45.4831	45.4831	69.7939	85.0385	85.0385	106.6840	106.6840	133.6220
	Present[b]	19.0649	45.4826	45.4826	69.7943	85.0380	85.0380	106.6836	106.6836	133.6212
0.1	Liew et al. (1995a)	19.0582	45.4495	45.4495	69.7189	84.9279	84.9279	106.5130	106.5130	–
	Present[c]	19.0584	45.4478	45.4478	69.7166	84.9263	84.9263	106.5154	106.5154	133.3705
0.1	Liew et al. (1995b)	19.0898	45.6193	45.6193	70.1038	85.4876	85.4876	107.3710	107.3710	–
	Present[a]	19.0840	45.5845	45.5845	70.0219	85.3654	85.3654	107.1775	107.1775	134.3586
0.2	Liew et al. (1993a)	17.4485	38.1519	38.1519	55.1504	65.1453	65.1453	78.6973	78.6973	94.7660
	Present[b]	17.4485	38.1521	38.1521	55.1500	65.1452	65.1452	78.6969	78.6969	94.7658
0.2	Liew et al. (1995b)	17.5264	38.4826	38.4826	55.7870	65.9961	65.9961	–	–	–
	Present[a]	17.5055	38.3847	38.3847	55.5860	65.7193	65.7193	79.4758	79.4758	95.8088

[a] Shear correction factor $K^2 = 0.86667$.
[b] Shear correction factor $K^2 = 5/6$.
[c] Shear correction factor $K^2 = \pi^2/12$.

Table 10
Comparison study of frequency parameters $\beta = \omega a^2\sqrt{\rho h/D}$ for square Mindlin plates with S–C–S–S boundaries

δ	Method	Mode sequences								
		1	2	3	4	5	6	7	8	9
0.001	Leissa (1973)	23.6463	51.6743	58.6464	86.1345	100.2698	113.2281	133.7910	140.8456	168.9585
	Liew et al. (1993a)	23.6456	51.6733	58.6452	86.1330	100.2680	113.2250	133.7870	140.8410	168.9540
	Present[a]	23.6461	51.6737	58.6455	86.1329	100.2679	113.2253	133.7874	140.8414	168.9533
0.1	Liew et al. (1993a)	22.3882	47.1037	52.1500	74.1049	85.8764	93.2273	109.2590	112.7410	134.0850
	Present[b]	22.3886	47.1039	52.1496	74.1051	85.8759	93.2267	109.2595	112.7410	134.0847
0.2	Liew et al. (1993a)	19.7037	38.9474	41.4474	56.8361	65.4463	67.9364	79.4849	80.4531	94.8943
	Present[b]	19.7032	38.9470	41.4472	56.8361	65.4459	67.9364	79.4849	80.4527	94.8942

[a] Shear correction factor $K^2 = 0.86667$.
[b] Shear correction factor $K^2 = 5/6$.

4.2. Comparison with known results

Since the present results are obtained based on using the exact characteristic equations for each case, the comparison with the other known results which are based on using the approximate methods may not be relevant. However to validate the accuracy of the present prediction a comparison has been carried out for thin ($\delta = 0.001$) square rectangular plate solutions.

In Leissa's well-known paper (Leissa, 1973), the exact characteristic equations and their vibration frequencies were presented for thin rectangular plates with two opposite edge simply supported. The first nine frequency parameters listed in Tables 9–14 for all considered six cases have been compared with those exact values (Leissa, 1973). They show good agreement.

In addition, it is not difficult to show that all exact characteristic equation formulas given for thick plate in present study lead to those given in (Leissa, 1973) by taking into account the relevant assumptions for

Table 11
Comparison study of frequency parameters $\beta = \omega a^2\sqrt{\rho h/D}$ for square Mindlin plates with S–C–S–C boundaries

δ	Method	Mode sequences								
		1	2	3	4	5	6	7	8	9
0.001	Leissa (1973)	28.9509	54.7431	69.3270	94.5853	102.2162	129.0955	140.2045	154.7757	170.3465
	Liew et al. (1993a)	28.9515	54.7418	69.3261	94.5834	102.2140	129.0910	140.2010	154.7700	170.3460
	Liew et al. (1995a)	28.9475	54.7467	69.3241	94.5804	102.2100	129.0940	140.1980	154.7750	–
	Present[a]	28.9505	54.7423	69.3257	94.5831	102.2141	129.0914	140.2002	154.7700	170.3410
0.1	Liew et al. (1993a)	26.6687	49.1131	59.2097	78.8127	86.8436	101.3720	112.0590	118.9220	134.5970
	Present[b]	26.6683	49.1129	59.2101	78.8129	86.8440	101.3717	112.0584	118.9220	134.5952
0.1	Liew et al. (1995a)	26.6479	49.0618	59.1189	78.6805	86.7242	101.1540	111.8520	118.6620	–
	Present[c]	26.6448	49.0625	59.1183	78.6831	86.7203	101.1523	111.8481	118.6574	134.3358
0.2	Liew et al. (1993a)	22.3596	39.8525	44.6155	58.5504	65.7701	70.5627	80.2942	82.1615	95.0285
	Present[b]	22.3593	39.8525	44.6154	58.5501	65.7703	70.5622	80.2939	82.1610	95.0283

[a] Shear correction factor $K^2 = 0.86667$.
[b] Shear correction factor $K^2 = 5/6$.
[c] Shear correction factor $K^2 = \pi^2/12$.

Table 12
Comparison study of frequency parameters $\beta = \omega a^2\sqrt{\rho h/D}$ for square Mindlin plates with S–F–F–F boundaries

δ	Method	Mode sequences								
		1	2	3	4	5	6	7	8	9
0.001	Leissa (1973)	11.6845	27.7563	41.1967	59.0655	61.8606	90.2941	94.4837	108.9185	115.6857
	Liew et al. (1993a)	11.6925	27.7602	41.1987	59.0656	61.8617	90.2931	94.4817	108.9170	115.6840
	Present[a]	11.6837	27.7523	41.1943	59.0587	61.8535	90.2885	94.4684	108.9084	115.6759
0.1	Liew et al. (1993a)	11.3727	26.1545	38.2862	53.2465	55.6231	78.3686	81.0758	92.2097	97.3548
	Present[b]	11.3731	26.1544	38.2860	53.2462	55.6233	78.3663	81.0755	92.2072	97.3551
0.2	Liew et al. (1993a)	10.6987	23.1531	32.7158	43.5743	45.3054	60.7375	62.3285	69.5787	72.7893
	Present[b]	10.6981	23.1532	32.7157	43.5740	45.3051	60.7370	62.3281	69.5788	72.7892

[a] Shear correction factor $K^2 = 0.86667$.
[b] Shear correction factor $K^2 = 5/6$.

Table 13
Comparison study of frequency parameters $\beta = \omega a^2 \sqrt{\rho h/D}$ for square Mindlin plates with S–F–S–F boundaries

δ	Method	Mode sequences								
		1	2	3	4	5	6	7	8	9
0.001	Leissa (1973)	9.6314	16.1348	36.7256	38.9450	46.7381	70.7401	75.2834	87.9867	96.0405
	Liew et al. (1993a)	9.6406	16.1417	36.7297	38.9474	46.7395	70.7394	75.2834	87.9865	96.0401
	Liew et al. (1995a)	9.6327	16.1368	36.7248	38.9455	46.7326	70.7355	75.2853	87.9875	–
	Present[a]	9.6311	16.1313	36.7161	38.9433	46.7317	70.7222	75.2692	87.9819	96.0288
0.1	Liew et al. (1993a)	9.4403	15.3897	33.8597	36.3576	42.7926	62.1499	66.1964	76.6355	82.4240
	Present[b]	9.4406	15.3892	33.8599	36.3569	42.7926	62.1466	66.1965	76.6329	82.4088
0.1	Liew et al. (1995a)	9.4354	15.3867	33.8429	36.3300	42.7551	62.0798	66.1362	76.5388	–
	Present[c]	9.4388	15.3837	33.8407	36.3338	42.7604	62.0840	66.1366	76.5404	82.3031
0.1	Liew et al. (1995b)	9.4462	15.3995	33.9129	36.4376	42.8874	62.3374	66.4096	76.9730	–
	Present[a]	9.4458	15.4054	33.9161	36.4246	42.8870	62.3304	66.3720	76.9042	82.7190
0.2	Liew et al. (1993a)	8.9833	14.0938	29.1361	31.2709	35.9599	49.5612	52.4796	59.6164	63.2681
	Present[b]	8.9830	14.0939	29.1363	31.2704	35.9599	49.5606	52.4793	59.6159	63.2657
0.2	Liew et al. (1995b)	9.0010	14.1224	29.2634	31.4722	36.1731	49.9353	52.9119		
	Present[a]	8.9997	14.1341	29.2558	31.4338	36.1646	49.8953	52.8012	60.1064	63.7961

[a] Shear correction factor $K^2 = 0.86667$.
[b] Shear correction factor $K^2 = 5/6$.
[c] Shear correction factor $K^2 = \pi^2/12$.

Table 14
Comparison study of frequency parameters $\beta = \omega a^2 \sqrt{\rho h/D}$ for square Mindlin plates with S–C–S–F boundaries

δ	Method	Mode sequences								
		1	2	3	4	5	6	7	8	9
0.001	Leissa (1973)	12.6874	33.0651	41.7019	63.0148	72.3976	90.6114	103.1617	111.8964	131.4287
	Liew et al. (1993a)	12.6854	33.0651	41.7020	63.0135	72.3955	90.6099	103.1580	111.8940	131.4250
	Present[a]	12.6862	33.0600	41.6993	63.0064	72.3896	90.6054	103.1439	111.8848	131.4175
0.1	Liew et al. (1993a)	12.2492	30.4083	38.6346	55.8018	62.7263	78.5285	85.8942	93.6852	105.6140
	Present[b]	12.2492	30.4086	38.6342	55.8017	62.7259	78.5265	85.8934	93.6825	105.6138
0.2	Liew et al. (1993a)	11.3619	25.7547	32.8934	44.7241	48.5022	60.7948	64.0419	70.0752	75.3031
	Present[b]	11.3619	25.7545	32.8937	44.7244	48.5026	60.7949	64.0421	70.0755	75.3026

[a] Shear correction factor $K^2 = 0.86667$.
[b] Shear correction factor $K^2 = 5/6$.

thin plates. This can be directly achieved for plate with no free edge by letting $K^2 \to \inf$, which suggests $C_1 = C_2 = 1$.

Further it is found that the first nine frequency parameters calculated for $\delta = 10^{-6}$ up to three decimal and more often up to four decimal figures are the same as those given in (Leissa, 1973). This in turn verifies that as δ gets insignificance the present exact characteristic equations given for thick plates have ability to predict the same results as those obtained in (Leissa, 1973) by using the exact characteristic equations of thin plates.

In Tables 9–14 the frequency parameters are also compared with those presented in Liew et al. (1993a) that used a shear correction factor $K^2 = 5/6$ for analysis with two dimensional Rayliegh–Ritz method. Further comparison studies have also been carried out in Tables 9 and 13 with existing values given in Liew et al. (1995a) and Liew et al. (1995b) obtained by using boundary characteristic orthogonal polynomials and three dimensional analysis, respectively. A shear correction factor of $K^2 = \pi^2/12$ was assumed in Liew et al. (1995a). The frequency parameters listed for S–C–S–C case in Table 11 are also compared with available data given in Liew et al. (1995a). It can be observed that for all six considered cases compared in Tables 9–14 the close agreement exist. This further justifies the validity of the present results.

5. Conclusions

In this work the Mindlin plate theory is used to investigate the free vibrations of thick rectangular plates. The exact characteristic equations are derived for the six cases having two opposite sides simply supported. The six cases considered are namely S–S–S–S, S–C–S–S, S–C–S–C, S–S–S–F, S–F–S–F and S–C–S–F plates. The transverse deflections are also given in closed form for all six cases, from which the modal shapes and counter plots at any desired frequency parameters can be graphically displayed.

Accurate frequency parameters are presented for different thickness ratios and aspect ratios for each case. These frequency parameters can be regarded as an exact database for each of considered cases and may be of worth to someone desiring to investigate the accuracy of an approximate method on some of these problems. The effect of boundary conditions, variation of aspect ratios and thickness ratios on the frequency values are examined and discussed in detail. Investigations are also carried out regarding nodal lines, obtaining additional results for other aspect ratios not included in presented tables, existence of the eigenvalues such that $\alpha_1 < m\pi$ and some specification of individual cases. Finally based on comparison with previously published results the validity of the presented results are established.

Appendix A. Different possible solutions for Eqs. (12a)–(12c)

In order to solve Eqs. (12a)–(12c) the method of separation of variables may be used. Thus, by selecting $W_i = f_i(X_1)g_i(X_2)$ $(i = 1,2,3)$ we obtain:

$$f_{i,11} = \pm\mu_i^2 f_i, \quad g_{i,22} = \pm\lambda_i^2 g_i \tag{A.1,A.2}$$

where μ_i^2 and λ_i^2 are separation constants. It can be easily shown that by examining the boundary conditions, a solution to the equations $f_{i,11} = \mu_i^2 f_i$ are not suitable for satisfying the boundary conditions when two opposite edges at $X_1 = 0$ and $X_1 = 1$ are simply supported. Hence, the following solutions to Eqs. (A.1) and (A.2) may be selected

$$f_i(X_1) = \tilde{a}_i \sin\mu_i X_1 + \tilde{b}_i \cos\mu_i X_1 \tag{A.3}$$

$$g_i(X_2) = \tilde{c}_i \sin\lambda_i X_2 + \tilde{d}_i \cos\lambda_i X_2 \tag{A.4}$$

$$g_i(X_2) = c_i^* \sinh\lambda_i X_2 + d_i^* \cosh\lambda_i X_2. \tag{A.5}$$

Close examination of Eqs. (11c)–(11e) reveals that

$$\alpha_1^2 > 0, \quad \alpha_2^2 > 0, \quad \alpha_3^2 > 0, \quad \text{for} \quad \beta > \frac{12K}{\delta^2}\sqrt{v_1}, \tag{A.6}$$

and

$$\alpha_1^2 > 0, \quad \alpha_2^2 < 0, \quad \alpha_3^2 < 0, \quad \text{for} \quad \beta < \frac{12K}{\delta^2}\sqrt{v_1}. \tag{A.7}$$

On assumption that $\alpha_1 > \mu_1$, $\alpha_2 > \mu_2$ and $\alpha_3 > \mu_3$ for conditions presented by expression (A.6), one set of solutions may be expressed as:

$$W_1 = [A_1 \sin(\lambda_1 X_2) + A_2 \cos(\lambda_1 X_2)] \sin(\mu_1 X_1) + [B_1 \sin(\lambda_1 X_2) + B_2 \cos(\lambda_1 X_2)] \cos(\mu_1 X_1), \tag{A.8}$$

$$W_2 = [A_3 \sin(\lambda_2 X_2) + A_4 \cos(\lambda_2 X_2)] \sin(\mu_2 X_1) + [B_3 \sin(\lambda_2 X_2) + B_4 \cos(\lambda_2 X_2)] \cos(\mu_2 X_1), \tag{A.9}$$

$$W_3 = [A_5 \sin(\lambda_3 X_2) + A_6 \cos(\lambda_3 X_2)] \cos(\mu_3 X_1) + [B_5 \sin(\lambda_3 X_2) + B_6 \cos(\lambda_3 X_2)] \sin(\mu_3 X_1), \tag{A.10}$$

where

$$\alpha_1^2 = \mu_1^2 + \eta^2 \lambda_1^2, \quad \alpha_2^2 = \mu_2^2 + \eta^2 \lambda_2^2, \quad \alpha_3^2 = \mu_3^2 + \eta^2 \lambda_3^2. \tag{A.11–A.13}$$

Keeping conditions same as given by expressions (A.6), the next three sets of solutions may be written as:

$$W_1 = [A_1 \sin(\lambda_1 X_2) + A_2 \cos(\lambda_1 X_2)] \sin(\mu_1 X_1) + [B_1 \sin(\lambda_1 X_2) + B_2 \cos(\lambda_1 X_2)] \cos(\mu_1 X_1), \tag{A.14}$$

$$W_2 = [A_3 \sin(\lambda_2 X_2) + A_4 \cos(\lambda_2 X_2)] \sin(\mu_2 X_1) + [B_3 \sin(\lambda_2 X_2) + B_4 \cos(\lambda_2 X_2)] \cos(\mu_2 X_1), \tag{A.15}$$

$$W_3 = [A_5 \sinh(\lambda_3 X_2) + A_6 \cosh(\lambda_3 X_2)] \cos(\mu_3 X_1) + [B_5 \sinh(\lambda_3 X_2) + B_6 \cosh(\lambda_3 X_2)] \sin(\mu_3 X_1), \tag{A.16}$$

where

$$\alpha_1 > \mu_1, \quad \alpha_2 > \mu_2, \quad \alpha_3 < \mu_3 \tag{A.17–A.19}$$

$$\alpha_1^2 = \mu_1^2 + \eta^2 \lambda_1^2, \quad \alpha_2^2 = \mu_2^2 + \eta^2 \lambda_2^2, \quad \alpha_3^2 = \mu_3^2 - \eta^2 \lambda_3^2, \tag{A.20–A.22}$$

$$W_1 = [A_1 \sin(\lambda_1 X_2) + A_2 \cos(\lambda_1 X_2)] \sin(\mu_1 X_1) + [B_1 \sin(\lambda_1 X_2) + B_2 \cos(\lambda_1 X_2)] \cos(\mu_1 X_1), \tag{A.23}$$

$$W_2 = [A_3 \sinh(\lambda_2 X_2) + A_4 \cosh(\lambda_2 X_2)] \sin(\mu_2 X_1) + [B_3 \sinh(\lambda_2 X_2) + B_4 \cosh(\lambda_2 X_2)] \cos(\mu_2 X_1), \tag{A.24}$$

$$W_3 = [A_5 \sin(\lambda_3 X_2) + A_6 \cos(\lambda_3 X_2)] \cos(\mu_3 X_1) + [B_5 \sin(\lambda_3 X_2) + B_6 \cos(\lambda_3 X_2)] \sin(\mu_3 X_1), \tag{A.25}$$

where

$$\alpha_1 > \mu_1, \quad \alpha_2 < \mu_2, \quad \alpha_3 > \mu_3 \tag{A.26–A.28}$$

$$\alpha_1^2 = \mu_1^2 + \eta^2 \lambda_1^2, \quad \alpha_2^2 = \mu_2^2 - \eta^2 \lambda_2^2, \quad \alpha_3^2 = \mu_3^2 + \eta^2 \lambda_3^2, \tag{A.29–A.31}$$

and

$$W_1 = [A_1 \sin(\lambda_1 X_2) + A_2 \cos(\lambda_1 X_2)] \sin(\mu_1 X_1) + [B_1 \sin(\lambda_1 X_2) + B_2 \cos(\lambda_1 X_2)] \cos(\mu_1 X_1), \tag{A.32}$$

$$W_2 = [A_3 \sinh(\lambda_2 X_2) + A_4 \cosh(\lambda_2 X_2)] \sin(\mu_2 X_1) + [B_3 \sinh(\lambda_2 X_2) + B_4 \cosh(\lambda_2 X_2)] \cos(\mu_2 X_1), \tag{A.33}$$

$$W_3 = [A_5 \sinh(\lambda_3 X_2) + A_6 \cosh(\lambda_3 X_2)] \cos(\mu_3 X_1) + [B_5 \sinh(\lambda_3 X_2) + B_6 \cosh(\lambda_3 X_2)] \sin(\mu_3 X_1), \tag{A.34}$$

where

$$\alpha_1 > \mu_1, \quad \alpha_2 < \mu_2, \quad \alpha_3 < \mu_3 \tag{A.35–A.37}$$

$$\alpha_1^2 = \mu_1^2 + \eta^2 \lambda_1^2, \quad \alpha_2^2 = \mu_2^2 - \eta^2 \lambda_2^2, \quad \alpha_3^2 = \mu_3^2 - \eta^2 \lambda_3^2. \tag{A.38–A.40}$$

To satisfy the boundary conditions when two opposite edges at $X_1 = 0$ and $X_1 = 1$ are simply supported we should write:

$$\mu_1 = \mu_2 = \mu_3 = m\pi. \tag{A.41}$$

It is not difficult to show that $\alpha_3 > \alpha_2$ by rewriting Eq. (11e) as:

$$\frac{\alpha_3^2}{\alpha_2^2} = \frac{12K^2}{\beta^2\delta^2}\alpha_1^2 \tag{A.42}$$

and showing that the right-hand side of Eq. (A.42) is always greater than unity. Thus, the set of solutions given by Eqs. (A14)–(A16) to maintain conditions as shown by expressions (A17)–(A19) may be eliminated.

As far as the conditions presented by expressions (A.7) are concerned, the set of solutions given by Eqs. (A.32), (A.33), (A.34) are valid by ignoring inequalities (A.36) and (A.37). Thus, there will exist three sets of solutions for $\beta > 12K\sqrt{\upsilon_1}/\delta^2$ and one set of solutions for $\beta < 12K\sqrt{\upsilon_1}/\delta^2$ if $\alpha_1 > \mu_1$. The solutions concerning $\alpha_1 < \mu_1$ have been dealt with separately in Appendix B.

Selecting $\upsilon = 0.3$, $K^2 = 0.86667$ and finding the values of $\beta = 12K\sqrt{\upsilon_1}/\delta^2$ for the values of $\delta =$ 0.01, 0.05, 0.1, 0.15 and 0.2 as listed in Tables 1–6, we obtain $\beta = 66091$, 2643.64, 660.91, 293.738 and 165.227, respectively. Close inspection of frequencies listed in Tables 1–6 reveals that within the range of frequencies considered for each value of δ, except three listed values of β, the rest of listed corresponding frequencies are less than the values of $12K\sqrt{\upsilon_1}/\delta^2$ calculated for each corresponding value of δ. This in turn suggests that the best set of solutions within the range of frequencies considered in Tables 1–6 is the set given by Eqs. (13a)–(13c). Obviously, for these three values of β appearing as β_{42} with corresponding values of $\delta = 0.2$ and $\eta = 2.5$ in Tables 1–3, inspection of values of α_2 and α_3 could lead to selection of appropriate sets of solutions.

In order to obtain the characteristic equations and the nondimensional transverse displacements from Eqs. (18)–(24) and (37)–(46c), respectively for $\beta > 12K\sqrt{\upsilon_1}/\delta^2$, depending on the values of α_2 and α_3 the following replacements could take place:

$$\alpha_2 > \mu_2, \quad \alpha_3 > \mu_3 \quad \text{(replacing } \lambda_2 \text{ and } \lambda_3 \text{ by } \mathrm{i}\lambda_2 \text{and } \mathrm{i}\lambda_3 \text{ respectively)}, \tag{A.43}$$

$$\alpha_2 < \mu_2, \quad \alpha_3 > \mu_3 \quad \text{(replacing } \lambda_3 \text{ by } \mathrm{i}\lambda_3\text{)}, \tag{A.44}$$

and

$$\alpha_2 < \mu_2, \quad \alpha_3 < \mu_3 \quad \text{(no modification is required)}. \tag{A.45}$$

Appendix B. On the existence of eigenvalues such that $\alpha_1 < m\pi$

In order to investigate the existence of eigenvalues such that $\alpha_1 < m\pi$, it is convenient to express α_2 and α_3 in terms of α_1. Upon making use of Eqs. (11c)–(11e), one may write

$$\alpha_2^2 = a_1\beta^2 - \alpha_1^2, \quad \alpha_3^2 = \frac{12K^2}{\beta^2\delta^2}\alpha_1^2(a_1\beta^2 - \alpha_1^2), \tag{B.1,B.2}$$

where a_1 is given by Eq. (58a). Thus $\tilde{\lambda}_1$, λ_2, λ_3, C_1 and C_2 are given by Eqs. (26), (25c), (25d), (11a), and (11b), respectively, may be written as

$$\tilde{\lambda}_1 = \frac{1}{\eta}\sqrt{-\alpha_1^2 + m^2\pi^2}, \quad \lambda_2 = \frac{1}{\eta}\sqrt{\alpha_1^2 - a_1\beta^2 + m^2\pi^2}, \tag{B.3,B.4}$$

$$\lambda_3 = \frac{K\alpha_1}{\eta\beta\delta}\sqrt{12(\alpha_1^2 - a_1\beta^2) + \frac{m^2\pi^2\beta^2\delta^2}{K^2\alpha_1^2}}, \tag{B.5}$$

$$C_1 = 1 - \frac{\beta^2\delta^2}{12K^2\alpha_1^2 v_1}, \quad C_2 = 1 - \frac{\beta^2\delta^2}{12K^2(a_1\beta^2 - \alpha_1^2)v_1}. \tag{B.6,B.7}$$

The nondimensional frequency parameter may also be solved in terms of α_1 by using Eq. (11c), to give

$$\beta^2 = \frac{2\left[a_1\alpha_1^2 + 1 - \sqrt{(a_1\alpha_1^2+1)^2 - (a_1^2 - a_2^2)\alpha_1^4}\right]}{(a_1^2 - a_2^2)}, \tag{B.8}$$

where a_2 is given by Eq. (58b). Investigation of the existence of eigenvalues may now be given below for each individual cases.

Case 1 S–S–S–S

Eq. (27) may be written as

$$f(\beta) = \sinh\tilde{\lambda}_1 \sinh\lambda_2 \sinh\lambda_3 = 0, \tag{B.9}$$

where for a given values of K, η, δ, v and m, $\tilde{\lambda}_1$, λ_2 and λ_3 are all functions of β according to Eqs. (B.3)–(B.5). At $\beta = 0$, $\alpha_1 = \alpha_2 = 0$, $\tilde{\lambda}_1 = \lambda_2 = m\pi/\eta$ and $\lambda_3 = \sqrt{12K^2 + m^2\pi^2\delta^2}/\eta\delta$. Therefore, $\sinh\tilde{\lambda}_1 = \sinh\lambda_2 > 0$, $\sinh\lambda_3 > 0$ and $f(0) > 0$. As β increases, $f(\beta)$ remains greater than zero and becomes zero at $\alpha_1 = m\pi$. The corresponding nondimensional frequency parameter β^* at $\alpha_1 = m\pi$ may be given by replacing α_1 by $m\pi$ in Eq. (B.8). Thus, $f(\beta) > 0$ for all β in the range $0 < \beta < \beta^*$, therefore no eigenvalues can exist.

Case 2. S–C–S–S

Eq. (28) can be rewritten as $f(\beta) = g(\beta)$, where

$$f(\beta) = C_2\left(\frac{\tanh\tilde{\lambda}_1}{\tilde{\lambda}_1} - \frac{\mu^2}{\eta^2\tilde{\lambda}_1\lambda_2\lambda_3}\frac{\tanh\tilde{\lambda}_1\tanh\lambda_2}{\tanh\lambda_3}\right), \tag{B.10}$$

$$g(\beta) = C_1\left(\frac{\tanh\lambda_2}{\lambda_2} - \frac{\mu^2}{\eta^2\tilde{\lambda}_1\lambda_2\lambda_3}\frac{\tanh\tilde{\lambda}_1\tanh\lambda_2}{\tanh\lambda_3}\right). \tag{B.11}$$

Comparing Eqs. (B.3) and (B.4), and taking into account the fact that for all $\beta > 0$, $\alpha_2^2 = a_1\beta^2 - \alpha_1^2 < 0$. Thus $\alpha_1^2 > a_1\beta^2$, and consequently $\lambda_2 > \tilde{\lambda}_1$ for all $\beta > 0$. Similarly, comparison of Eqs. (B.6) and (B.7) clears that $C_2 > C_1$ for all $\beta > 0$. At $\beta = 0$, $C_2 = C_1 = 1$ and $f(0) = g(0)$ which is a trivial root. As a result of $C_2 > C_1$ one may conclude that the second term on the right-hand side of Eq. (B.10) is greater than the second term on the right-hand side of Eq. (B.11) for all $\beta > 0$. Furthermore due to the fact that $\lambda_2 > \tilde{\lambda}_1$ it is not difficult to show that $C_2\tanh\tilde{\lambda}_1/\tilde{\lambda}_1 > C_1\tanh\lambda_2/\lambda_2$ as β increases. Thus, $f(\beta) > g(\beta)$ for all $\beta > 0$, therefore no eigenvalues can exist.

Case 3. S–C–S–C

Consider first the x_2-symmetric modes. Eq. (35c) is rewritten as $f(\beta) = g(\beta)$, where

$$f(\beta) = C_1\left(\frac{\tilde{\lambda}_1}{2}\tanh\frac{\tilde{\lambda}_1}{2} - \frac{\mu^2}{2\eta^2\lambda_3}\tanh\frac{\lambda_3}{2}\right), \tag{B.12}$$

$$g(\beta) = C_2\left(\frac{\lambda_2}{2}\tanh\frac{\lambda_2}{2} - \frac{\mu^2}{2\eta^2\lambda_3}\tanh\frac{\lambda_3}{2}\right). \tag{B.13}$$

But $\lambda_2 > \tilde{\lambda}_1$ and $C_2 > C_1$ for all $\beta > 0$. For $\beta = 0, f(0) = g(0)$, which is a trivial root. As β increases, $\tilde{\lambda}_1/2$ and $\tanh \tilde{\lambda}_1/2$ both decrease, and $\lambda_2/2$ and $\tanh(\lambda_2/2)$ both increase. At $\alpha_1 = m\pi$, $\tilde{\lambda}_1/2 = \tanh(\tilde{\lambda}_1/2) = 0$. Thus $f(\beta) < g(\beta)$ for all β in the range $0 < \beta < \beta^*$, and no x_2-symmetric eigenvalues can exist.

Eq. (35c,d) for the x_2-antisymmetric modes is similar to the Eq. (28) of case 2. Therefore, no x_2-antisymmetric eigenvalues can exist. The proof is the same as case 2.

Case 4. S–S–S–F

Eq. (30) may be rewritten as $f(\beta) = g(\beta)$, where

$$f(\beta) = 2(C_1 - C_2)\eta^2\mu^2\lambda_3(1-\nu)\tanh\lambda_3 - C_2L_1L_2\tanh\lambda_2/\lambda_2, \tag{B.14}$$

$$g(\beta) = C_1L_3L_4\tanh\tilde{\lambda}_1/\tilde{\lambda}_1. \tag{B.15}$$

For $\beta = 0$,

$$f(0) = g(0) = 2m^3\pi^3\eta(1-\nu)\tanh(m\pi/\eta) > 0. \tag{B.16}$$

Furthermore, letting $\alpha_1 = m\pi\sqrt{1-\nu}$ gives $f(\beta_1) > 0$ and $g(\beta_1) = 0$, where β_1 is the corresponding nondimensional frequency parameter at $\alpha_1 = m\pi\sqrt{1-\nu}$. Therefore, a root of equation (30) will exist in the interval $\beta_1 < \beta < \beta^*$ if

$$f(\beta^*) < g(\beta^*). \tag{B.17}$$

For a given values of K, η, δ and ν expression (B.17) is a function of m only. Thus the lowest value of m satisfying the condition for the existence of eigenvalues may be estimated. The nondimensional transverse deflection may also be obtained from Eqs. (41) and (42a)–(42c) by simply replacing λ_1 and L_4 by $\mathrm{i}\tilde{\lambda}_1$ and $\widetilde{L}_4$, respectively, where $\mathrm{i} = \sqrt{-1}$.

Case 5. S–F–S–F

Consider first the x_2-symmetric modes. Eq. (36c) is rewritten as $f(\beta) = g(\beta)$, where

$$f(\beta) = 2(C_1 - C_2)\eta^2\mu^2\tilde{\lambda}_1\lambda_3(1-\nu)\frac{\tanh(\tilde{\lambda}_1/2)\tanh(\lambda_2/2)}{\tanh(\lambda_3/2)} - C_2L_1L_2\frac{\tilde{\lambda}_1}{\lambda_2}\tanh\frac{\tilde{\lambda}_1}{2},$$

$$g(\beta) = C_1L_3L_4\tanh(\lambda_2/2). \tag{B.18,B.19}$$

For $\beta = 0$,

$$f(0) = g(0) = 2m^4\pi^4(1-\nu)\tanh\frac{m\pi}{2\eta} > 0. \tag{B.20}$$

Furthermore, letting $\alpha_1 = m\pi\sqrt{1-\nu}$ gives $f(\beta_1) > 0$ and $g(\beta_1) = 0$. Thus a root of equation (36c) will exist in the interval $\beta_1 < \beta < \beta^*$ if $f(\beta^*) < g(\beta^*)$. Upon letting $\alpha_1 = m\pi$, $f(\beta) = 0$ and $g(\beta) > 0$. Therefore, the x_2-symmetric eigenvalues will always exist, and they will exist in the interval $\beta_1 < \beta < \beta^*$.

Eq. (36c,d) for the x_2-antisymmetric modes can be rewritten as $f(\beta) = g(\beta)$, where

$$f(\beta) = 4(C_1 - C_2)\eta^2\mu^2\lambda_3(1-\nu)\tanh\frac{\lambda_3}{2} - 2C_2L_1L_2\frac{\tanh(\lambda_2/2)}{\lambda_2}, \tag{B.21}$$

$$g(\beta) = 2C_1L_3L_4\frac{\tanh(\tilde{\lambda}_1/2)}{\tilde{\lambda}_1}. \tag{B.22}$$

For $\beta = 0$,

$$f(0) = g(0) = 4m^3\pi^3\eta(1-\nu)\tanh\left(\frac{m\pi}{2\eta}\right) > 0. \tag{B.23}$$

At $\alpha_1 = m\pi\sqrt{1-\nu}$, $f(\beta_1) > 0$ and $g(\beta_1) = 0$. Thus a root of equation (36c,d) will exist in the interval $\beta_1 < \beta < \beta^*$ if $f(\beta^*) < g(\beta^*)$. The nondimensional transverse deflection for both x_2-symmetric and x_2-antisymmetric modes may also be obtained from Eqs. (43) and (44a)–(44f) by simply replacing λ_1 and L_4 by $\mathrm{i}\tilde{\lambda}_1$ and $\widetilde{L}_4$, respectively, where $\mathrm{i} = \sqrt{-1}$.

Case 6. S–C–S–F

Eq. (33) may be rewritten as $f(\beta) = g(\beta)$, where

$$\begin{aligned} f(\beta) = {} & \lambda_3\eta^2[2(C_1 - C_2)^2\mu^4(1-\nu) + C_1^2 L_3\widetilde{L}_4 - C_2^2 L_1 L_2]\cosh\tilde{\lambda}_1\cosh\lambda_2\cosh\lambda_3 \\ & + (C_2 - C_1)C_2\frac{\mu^2}{\lambda_2}\{[L_1L_2 - 2(1-\nu)\lambda_2^2\lambda_3^2\eta^4]\sinh\lambda_2\sinh\lambda_3 \\ & + \lambda_2\lambda_3\eta^2[L_1(1-\nu) - 2L_2]\}\cosh\tilde{\lambda}_1 \\ & + (C_2 - C_1)C_1\frac{\mu^2}{\tilde{\lambda}_1}\{[L_3\widetilde{L}_4 + 2(1-\nu)\tilde{\lambda}_1^2\lambda_3^2\eta^4]\sinh\tilde{\lambda}_1\sinh\lambda_3 \\ & - \tilde{\lambda}_1\lambda_3\eta^2[L_3(1-\nu) + 2\widetilde{L}_4]\}\cosh\lambda_2 + C_1C_2\lambda_3\eta^2(L_2L_3 - L_1\widetilde{L}_4)\cosh\lambda_3, \end{aligned} \tag{B.24}$$

$$g(\beta) = C_1C_2\lambda_3\eta^2\left(L_3\widetilde{L}_4\lambda_2^2 - L_1L_2\tilde{\lambda}_1^2\right)\frac{\sinh\tilde{\lambda}_1}{\tilde{\lambda}_1}\frac{\sinh\lambda_2}{\lambda_2}\cosh\lambda_3. \tag{B.25}$$

For $\beta = 0$

$$f(0) = g(0) = 4m^4\pi^4\eta(1-\nu)\sqrt{m^2\pi^2\delta^2 + 12K^2}\sinh^2\frac{m\pi}{\eta}\cosh\frac{\sqrt{m^2\pi^2\delta^2 + 12K^2}}{\eta\delta}. \tag{B.26}$$

Furthermore, letting $\alpha_1 = m\pi\sqrt{1-\nu}$ gives $f(\beta_1) > g(\beta_1)$. Therefore, a root of equation (33) will exist in the interval $\beta_1 < \beta < \beta^*$ if $f(\beta^*) < g(\beta^*)$. The nondimensional transverse deflection can also be deduced from Eqs. (45), (46a)–(46c) by simply replacing λ_1 and L_4 by $\mathrm{i}\tilde{\lambda}_1$ and $\widetilde{L}_4$, respectively, where $\mathrm{i} = \sqrt{-1}$.

References

Al Janabi, B.S., Hinton, E., Vuksanovic, D.J., 1989. Free vibration of Mindlin plates using the finite element methods, Part I: square plates with various edge conditions. Engineering Computers 6, 90–96.

Chen, C.C., Liew, K.M., Lim, C.W., Kitipornchai, S., 1997. Vibration analysis of symmetrically laminated thick rectangular plates using the higher-order theory and p-Ritz method. Journal of Acoustical Society of America 102, 1600–1611.

Cheung, Y.K., Chakrabarti, S., 1972. Free vibration of thick layered rectangular plates by a finite layer method. Journal of Sound and Vibration 21, 277–284.

Cheung, Y.K., Zhou, D., 2000. Vibrations of moderately thick rectangular plates in terms of a set of static Timoshenko beam functions. Computers and Structures 78, 757–768.

Dawe, D.J., 1987. Finite strip models for vibration of Mindlin plates. Journal of Sound and Vibration 59, 441–452.

Dawe, D.J., Roufaeil, O.L., 1980. Rayliegh–Ritz vibration analysis of Mindlin plates. Journal of Sound and Vibration 69, 345–359.

Leissa, A.W., 1969. Vibration of plates. NASA SP-160.

Leissa, A.W., 1973. The free vibration of rectangular plates. Journal of Sound and Vibration 31, 257–293.

Leissa, A.W., 1977. Recent research in plate vibrations: classical theory. The Shock and Vibration Digest 9 (10), 13–24.

Leissa, A.W., 1978. Recent research in plate vibrations, 1973–1976: complicating effects. The Shock and Vibration Digest 10 (12), 21–35.

Leissa, A.W., 1981a. Plate vibration research, 1976–1980: classical theory. The Shock and Vibration Digest 13 (9), 11–22.

Leissa, A.W., 1981b. Plate vibration research, 1976–1980: complicating effects. The Shock and Vibration Digest 13 (10).

Leissa, A.W., 1987a. Recent studies in plate vibrations, 1981–1985. Part I: classical theory. The Shock and Vibration Digest 19 (2), 11–18.

Leissa, A.W., 1987b. Recent studies in plate vibrations, 1981–1985. Part II: complicating effects. The Shock and Vibration Digest 19 (3), 10–24.

Liew, K.M., Teo, T.M., 1999. Three-dimensional vibration analysis of rectangular plates based on differential quadrature method. Journal of Sound and Vibration 220, 577–599.

Liew, K.M., Xiang, Y., Kitipornchai, S., 1995. Research on thick plate vibration: a literature survey. Journal of Sound and Vibration 180, 163–176.

Liew, K.M., Xiang, Y., Kitipornchai, S., 1993a. Transverse vibration of thick rectangular plates-I. Comprehensive sets of boundary conditions. Computers and Structures 49, 1–29.

Liew, K.M., Hung, K.C., Lim, M.K., 1993b. A continuum three -dimensional vibration analysis of thick rectangular plate. International Journal of Solids and Structures 24, 3357–3379.

Liew, K.M., Hung, K.C., Lim, M.K., 1994. Three-dimensional vibration of rectangular plates: variance of simply support conditions and influence of in-plane inertia. International Journal of Solids and Structures 31, 3233–3247.

Liew, K.M., Hung, K.C., Lim, M.K., 1995a. Vibration of Mindlin plates using boundary characteristic orthogonal polynomials. Journal of Sound and Vibration 182, 77–90.

Liew, K.M., Hung, K.C., Lim, M.K., 1995b. Three-dimensional vibration of rectangular plates: effects of thickness and edge constraints. Journal of Sound and Vibration 182, 709–727.

Liew, K.M., Wang, C.M., Xiang, Y., Kitipornchai, S., 1998. Vibration of Mindlin plates: Programming the p-Ritz Method. Elsevier, Oxford, UK, 202p.

Lim, C.W., liew, K.M., Kitipornchai, S., 1998a. Numerical aspects for free vibration of thick plates. Part I: formulation and verification. Computer Methods in Applied Mechanics and Engineering 156, 15–29.

Lim, C.W., Kitipornchai, S., Liew, K.M., 1998b. Numerical aspect for free vibration of thick plates. Part II: numerical efficiency and vibration frequencies. Computer Methods in Applied Mechanics and Engineering 156, 31–44.

Gorman, D.J., 2000. Free vibration analysis of completely free rectangular plates by the superposition-Galerkin method. Journal of Sound and Vibration 237 (5), 901–914.

Gorman, D.J., 1996. Accurate free vibration analysis of clamped Mindlin plates using the method of superposition. Journal of Sound and Vibration 198, 341–353.

Malik, M., Bert, C.W., 1998. Three-dimensional elasticity solutions for free vibrations of rectangular plates by the differential quadrature method. International Journal of Solids and Structures 35, 299–318.

Mindlin, R.D., 1951. Influence rotatory inertia and shear in flexural motion of isotropic, elastic plates. ASME Journal of Applied Mechanics 18, 31–38.

Mindlin, R.D., Schaknow, A., Deresiewicz, H., 1956. Flexural vibration of rectangular plates. ASME Journal of Applied Mechanics 23, 430–436.

Mikami, T., Yoshimura, J., 1984. Application of the collocation method to vibration analysis of rectangular Mindlin plates. Computers and Structures 18, 425–431.

Srinvas, S., Rao, C.V.J., Rao, A.K., 1970. An exact analysis for vibration of simply-supported homogeneous and laminated thick rectangular plates. Journal of Sound and Vibration 12, 187–199.

Wittrick, W.H., 1987. Analytical three-dimensional elasticity solutions to some plate problems, and some observations on Mindlin's plate theory. International Journal of Solids and Structures 23, 441–464.

Zhou, D., Cheung, Y.K., Au, F.T.K., Lo, S.H., 2002. Three-dimensional vibration analysis of thick rectangular plates using Chebyshev polynomial and Ritz method. International Journal of Solids and Structures 39, 6339–6353.